Elsevier Editorial System(tm) for Journal of Environmental Management

Manuscript Draft

Manuscript Number:

Title: Anaerobes supplemented with solely/dual nano-particles for bio-(H2&char) production from black liquor

Article Type: Research Article

Keywords: nutrient limitations; total reducing sugars; total phenolic compounds; enzymatic activities; extracellular polymeric substances

Corresponding Author: Dr. Mohamed El Qelish, PhD

Corresponding Author's Institution: National Research Centre

First Author: Mohamed El Qelish, PhD

Order of Authors: Mohamed El Qelish, PhD; Aida Galal; Zhong Yu; Mohamed Hassan; Hala Salah; Mohamed Hasanin; Fangang Meng; Ahmed Tawfik

Abstract: Simultaneous bio- (H2&char) production and treatment of black liquor (BL) rich of phenolic compounds was extensively investigated in batch anaerobic assays and pyrolysis experiments. The anaerobes were loaded with 50 mg/gVS of the solely nanoparticles i.e. graphene (nG), graphene oxide (nGO), magnetite (nM), hydoxyapetite (nHap) and dual-nanoparticles of graphene/magnetite (nG/M) and graphene/hydroxyapatite (nG/Hap). Supplementation with solely nanoparticles enhanced the H2 production and hydrogenase enzyme (HE) activities. However, the H2 yield (HY) was maximized at a level of 115.9±12.2 ml /gCODs removed, 190.6 ±9.8 mL/g carbohydrate removed and 365.4 ±14.3 mL/g protein removed for nG/Hap due to an increase of enzymatic activities of the α-amylase, α-xylanase, CM-cellulase, polygalacturonase and protease by values of 52.5±1.6%, 26.4±0.9%, 32.7±1.4%, 0.7±0.04% and 29.2±1.5%, respectively. Moreover, the half maximal inhibitory concentration (IC50) was significantly ($P \leq 0.5$) reduced from 49.1±2.8 µg gallic acid equivalent/mL for BL to 13.1±2.8 µg gallic acid equivalent/mL for anaerobes supplemented with nG/Hap. Moreover, addition of nG/Hap reduced the lag phase from 72 hrs for control to 12.0 h, due to a high activity of HE (0.28 ± 0.004 mg M.B reduced/min). This indicates that the addition of nG/Hap rich of calcium ions accelerated the biodegradation activities and surprisingly the antioxidants activities -ABTS (Scavenging %) were significantly ($P<0.5$) increased from 31.9±2.9 to 89.9±0.28% due to the removal of total phenolic compounds (TPC) by a value of 45.9±1.2%. Microbial community analysis revealed that dual nanoparticles inhibited the competitors and promoted the cooperators for the hydrogen producers, i.e., Firmicutes. The digestate resulted from fermentation of sludge, BL and nG/Hap were further pyrolyzed for bio-char production at temperature of 550 °C for 1.0 h. The bio-char exhibited a specific surface area of 2.4 ± 0.95 m2/g, density of 1.63 ± 0.18 g/cm3, pore volume of 0.2 ± 0.06 cm3/g and yield (33±5.2%). The maximum overall profit from both H2 and bio-char was 3000 $/m3.

Anaerobes supplemented with solely/dual nano-particles for bio-(H_2&char) production from black liquor

Mohamed El-Qelish[1], Aida Galal[1], Zhong Yu[2], Mohamed A. Hassan[3], H. A. Salah[4], Mohamed S. Hasanin[5], Fangang Meng[2], Ahmed Tawfik[1♥]

[1] National Research Centre, Water Pollution Research Department, 12622, Dokki, Cairo, Egypt

[2]School of Environmental Science and Engineering, Sun Yat-sen University, Guangzhou 510006, PR China

[3]Agricultural Research Center, Nanotechnology and Advanced Material Central Lab., Giza, Egypt

[4]National Research Centre, Molecular Biology Department, 12622, Dokki, Cairo, Egypt

[5]National Research Centre, Cellulose and Paper Department, 12622, Dokki, Cairo, Egypt

Corresponding author: Mohamed El Qelish
qelish88@yahoo.com, mm9283807@gmail.com

Water Pollution Research Department
National Research Centre
33 El Buhouth St., Dokki
Cairo, Egypt
Post Code 12622
Tel: +2 0100 675 8548

♥ Corresponding author: qelish88@yahoo.com, mm9283807@gmail.com (Mohamed El Qelish)

***Cover Letter**

Water Pollution Research Department
National Research Centre
33 El Buhouth St., Dokki
Cairo, Egypt
Post Code 12622

Dear Editor-in-Chief- Journal of Environmental Management

I am pleased to submit an original research manuscript entitled "*Anaerobes supplemented with solely/dual nano-particles for bio-(H_2&char) production from black liquor*" for consideration in the *Journal of Environmental Management*. This manuscript is an original research work of the authors and all the authors mutually agree for its submission to the *Journal of Environmental Management*. It has not previously been submitted to the *Journal of Environmental Management* nor has been published or undergoing review elsewhere.

Hydrogen fermentation of black liquor has got recently a great attention due to its high caloric value and as a clean biofuel. However, up-to- date the impact of immobilization of anaerobes on the solely and dual nanoparticles for bio-H_2 production from black liquor particularly on the enzymatic activities degrading proteins, carbohydrates, secretion of extracellular polymeric substances, ammonification, IC_{50} and ABST was not carried out, which extensively hereby addressed. Moreover, the immobilization of anaerobes on hydroxyapatite (nHap) and/or combined with Graphene is hereby investigated, where the nHap is rich with useful ions of phosphorus (P) and calcium (Ca) for micro-organisms. To our knowledge, there is no data in literature studying the impact of addition of nHap on the hydrogen producing bacteria from black liquor (BL).
Therefore, the main objectives of this study are to investigate the impact of immobilization of anaerobes on the solely/dual nano-particles for mitigation the inhibition effect of phenolic compounds and promote the antioxidant activities, enzymatic activities for carbohydrates and proteins degradation, extracellular polymeric substances secretion and ammonification process during fermentation of black liquor. Meanwhile, the high throughput 16S rRNA sequencing was conducted to uncover bacterial community shift induced by the nanoparticles. The correlations between the community members were identified to further explore the effect of bacterial responses to nanoparticles on the overall hydrogen production of the anaerobes. Moreover, the bio-char production was assessed along with the cost-benefit analysis of the integrated process.

We have no conflicts of interests to disclose.

Thank you for considering our manuscript.

Yours sincerely,
Mohamed El-Qelish

Graphical abstract

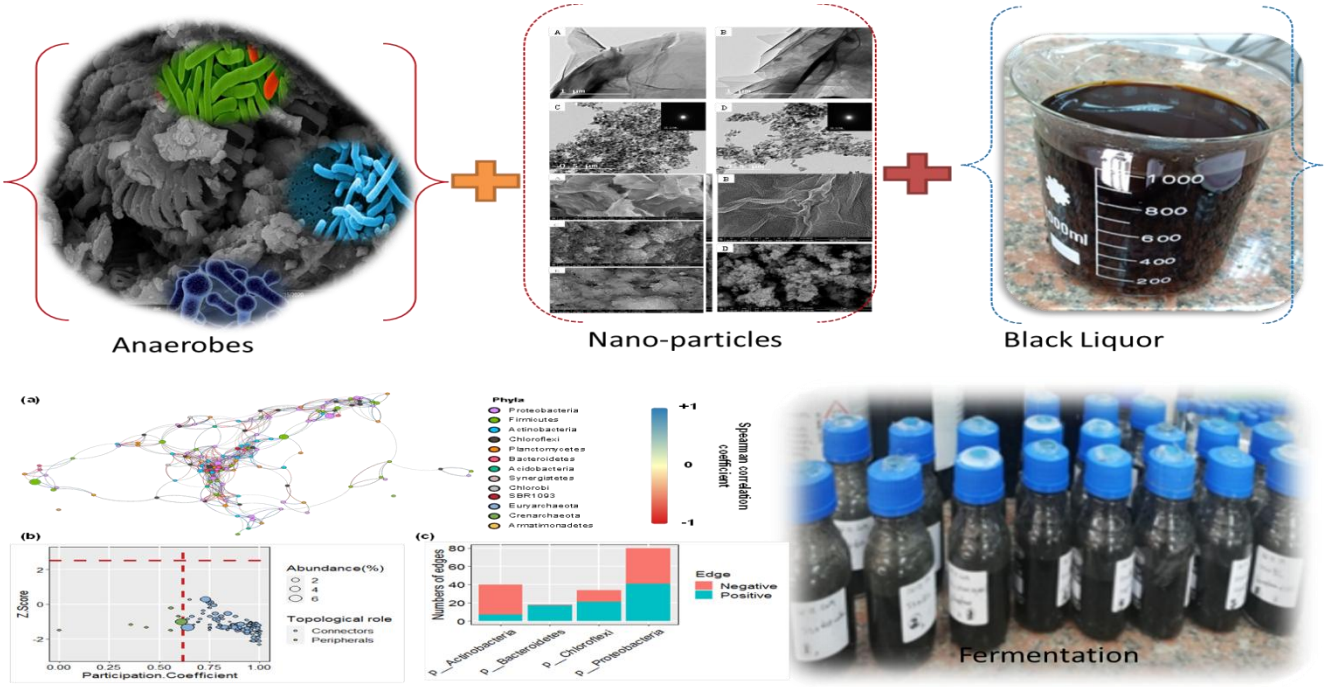

Highlights

- Immobilization of anaerobes on the solely and dual nano-particles improved HY
- nGraphene/hydroxyapatite reduces the inhibition effect of phenolic compounds
- Antioxidant activities was increased by supplementation of anaerobes with nano-particles
- Enzymatic activities were enhanced due to supplementation of dual nano-particles
- Ammonification and extracellular polymeric substances was maximized with nPS

Anaerobes supplemented with solely/dual nano-particles for bio-(H_2&char) production from black liquor

Mohamed El-Qelish[1], Aida Galal[1], Zhong Yu[2], Mohamed A. Hassan[3], H. A. Salah[4], Mohamed S. Hasanin[5], Fangang Meng[2], Ahmed Tawfik[1♥]

[1] National Research Centre, Water Pollution Research Department, 12622, Dokki, Cairo, Egypt

[2]School of Environmental Science and Engineering, Sun Yat-sen University, Guangzhou 510006, PR China

[3]Agricultural Research Center, Nanotechnology and Advanced Material Central Lab., Giza, Egypt

[4]National Research Centre, Molecular Biology Department, 12622, Dokki, Cairo, Egypt

[5]National Research Centre, Cellulose and Paper Department, 12622, Dokki, Cairo, Egypt

Abstract

Simultaneous bio- (H_2&char) production and treatment of black liquor (BL) rich of phenolic compounds was extensively investigated in batch anaerobic assays and pyrolysis experiments. The anaerobes were loaded with 50 mg/gVS of the solely nanoparticles i.e. graphene (nG), graphene oxide (nGO), magnetite (nM), hydoxyapetite (nHap) and dual-nanoparticles of graphene/magnetite (nG/M) and graphene/hydroxyapatite (nG/Hap). Supplementation with solely nanoparticles enhanced the H_2 production and hydrogenase enzyme (HE) activities. However, the H_2 yield (HY) was maximized at a level of 115.9±12.2 ml /gCODs $_{removed}$, 190.6 ±9.8 mL/g carbohydrate $_{removed}$ and 365.4 ±14.3 mL/g protein $_{removed}$ for nG/Hap due to an increase of enzymatic activities of the α-amylase, α-xylanase, CM-cellulase, polygalacturonase and protease by values of 52.5±1.6%, 26.4±0.9%, 32.7±1.4%, 0.7±0.04% and 29.2±1.5%, respectively. Moreover, the half maximal inhibitory concentration (IC_{50}) was significantly ($P \leq 0.5$) reduced from 49.1±2.8 µg gallic acid equivalent/mL for BL to 13.1±2.8 µg gallic acid equivalent/mL for anaerobes supplemented with nG/Hap. Moreover, addition of nG/Hap reduced the lag phase from 72 hrs for control to 12.0 h, due to a high activity of HE (0.28 ± 0.004 mg M.B reduced/min). This indicates that the addition of nG/Hap rich of calcium ions accelerated the biodegradation activities and surprisingly the antioxidants activities -ABTS (Scavenging %) were significantly ($P<0.5$) increased from 31.9±2.9 to 89.9±0.28% due to the removal of total

♥ Corresponding author: qelish88@yahoo.com, mm9283807@gmail.com (Mohamed El Qelish)

phenolic compounds (TPC) by a value of 45.9±1.2%. Microbial community analysis revealed that dual nanoparticles inhibited the competitors and promoted the cooperators for the hydrogen producers, i.e., *Firmicutes*. The digestate resulted from fermentation of sludge; BL and nG/Hap were further pyrolyzed for bio-char production at temperature of 550 °C for 1.0 h. The bio-char exhibited a specific surface area of 2.4 ± 0.95 m^2/g, density of 1.63 ± 0.18 g/cm^3, pore volume of 0.2 ± 0.06 cm^3/g and yield (33±5.2%). The maximum overall profit from both H_2 and bio-char was 3000 $\$/m^3$.

Keywords: *nutrient limitations; total reducing sugars; total phenolic compounds; enzymatic activities; extracellular polymeric substances*

1. Introduction

Agriculture wastes such as rice straw (RS) and sugar cane bagasse (SCB) are abundant and cause severe environmental problems due to a lack of proper management and financial support in developing countries. The RS and SCB are partially utilized for ethanol production and paper making industry. However, the chemical pulping process of RS and SCB produces considerable quantities of black liquor (BL) rich of phenolic compounds and non-biodegradable organics. Uncontrolled discharge and /or dumping of BL onto the environment cause severe health problems and water pollution. Fortunately, the BL is rich of carbohydrates, sugars, proteins and phosphorous, which can be easily utilized by micro-organisms to produce valuable products. Nevertheless, physio-chemical treatment processes have been previously employed for treatment of BL i.e. dissolved air flotation (Miranda et al., 2009), coagulation and precipitation (Rodrigues et al., 2008), adsorption (Sari et al., 2018), photocatalytic oxidation (Ksibi et al., 2003), fenton and photo-fenton reactions (Torrades et al., 2008), membrane filtration (Kevlich et al., 2017) and ozonation (Ko et al., 2009). Those technologies are consuming energy, chemicals and produce high volumes of sludge which needs further treatment processes. Aerobic treatment processes have been also attempted for treatment of BL and/or pulp –paper mill industry (Miao et al., 2009). The activated sludge process suffered and failed in the treatment of such wastewater due to their toxicity and aerobic bacteria are very sensitive to high content of phenolic compounds (Morales et al., 2015). Moreover, filamentous bacteria are dominated in the activated sludge units treating pulp and paper mill wastewater causing sludge bulking and poor removal efficiency of pollutants (Van Der Waarde et al., 2002). However, integration of anaerobic –

aerobic process was successfully employed and minimized the cost and the sludge production for the treatment of black liquor (BL) (Kortekaas and Field, 1998). To our knowledge the hydrogen fermentative of BL is scarce in literature.

Hydrogen fermentation of BL has recently got a great attention due to its high caloric value and as a clean biofuel. The hydrogen is an eco-friendly energy candidate and could be utilized for electricity generation using fuel cell. In addition, it could be used as a feedstock for many industries such as bio-fertilizers production by combination with the nitrogen from air. Hydrogen could substitute fossil fuels, minimizing the CO_2 emission. Hydrogen production from BL has been attempted by electrolysis (Nong et al., 2016; Roy Ghatak, 2006), supercritical water gasification & syngas chemical looping (Darmawan et al., 2019) and gasification (Andersson and Harvey, 2006). Hydrogen fermentative process is still the promising approach and eco-friendly technology where the cost and excess sludge is kept quite low. Anaerobic technology for H_2 production from BL is very competitive technology particularly for the countries suffering from a lack of financial support and fossil fuels. The H_2 production (HP) still does not take that great attention from the decision makers in the developing countries due to the relatively low production and yield of 55.4 ml/g-COD $_{removed}$ (Vaez et al., 2017). Moreover, it is hardly to find a literature concerning H_2 production from alkaline and nutrients deficient BL using anaerobes which are comprehensively addressed in this research work.

Several attempts have been tried to increase the H_2 production (HP) and yield (HY) from low value substrates, i.e. HP from industrial wastewater containing mono-ethylene glycol was significantly increased by 41, 30, and 29%, for anaerobes individually supplemented with α-Fe_2O_3 (200 mg/l), NiO (20 mg/l), and ZnO NPs (10 mg/l), respectively (Elreedy et al., 2017). Further improvement of HY was occurred with the immobilization of anaerobes on dual and multi-NPs due to the increase of *Clostridiales* (belonging to family *Clostridiaceae*; > 83%) in the reaction medium (Elreedy et al., 2019). Addition of hematite nanoparticles to the anaerobes fed with sucrose wastewater increased the hydrogen production rate (HPR) from 3.87 to 5.9 l/L.d (Salem et al., 2017). Mixed culture bacteria supplemented with 100 mg/l magnetite/graphene oxide (MGO) and fed with gelatinous wastewater industry promoted HY up to 112.4 ± 10.5 ml H_2/gCOD $_{removed}$ and provided degradation efficiency of 80.8 ± 7.6% for carbohydrates, 34.4 ± 2.3% for proteins and 31.4 ± 2.2% for lipids due to the enhancement of *Proteobacteria, Firmicutes, Clostridia* and *Bacilli activities* (Mostafa et al., 2016). $NiCo_2O_4$-graphene nano-

composites decorated with NF exhibited HPR of 0.14 ± 0.003 l/l .d which was 3.2 times higher than control samples (Jayabalan et al., 2020).

Up-to- date, the impact of immobilization of anaerobes on the solely and dual nanoparticles for bio-H_2 production from BL particularly on the enzymatic activities degrading proteins, carbohydrates, secretion of extracellular polymeric substances (EPS), ammonification, IC_{50} and ABST was not carried which extensively hereby addressed. Moreover, the immobilization of anaerobes on hydroxyapatite (nHap) and/or combined with graphene is hereby investigated, where the nHap is rich with useful ions of phosphorus (P) and calcium (Ca) for micro-organisms. To our knowledge, the nG/Hap was only studied for the removal of methylene blue (MB) dye from wastewater (Hassan et al., 2018), $NiFe_2O_4$/hydroxyapatite/graphene for removal of cadmium (Cd^{2+}) from wastewater (Kahrizi et al., 2018), biomedical applications (Turon et al., 2017), capture of strontium (Wen et al., 2014), photocatalyst and adsorption of Pb(II) ions (Bharath and Ponpandian, 2015; Safatian et al., 2019) and there is no data in literature studying the impact of addition of nHap on the hydrogen producing bacteria from BL.

Therefore, the main objectives of this study are to investigate the impact of immobilization of anaerobes on the solely/dual nano-particles for mitigation the inhibition effect of phenolic compounds and promote the antioxidant activities, enzymatic activities for carbohydrates and proteins degradation, extracellular polymeric substances secretion and ammonification process during fermentation of black liquor (BL). Meanwhile, the high throughput 16S rRNA sequencing was conducted to uncover bacterial community shift induced by the nanoparticles. The correlations between the community members were identified to further explore the effect of bacterial responses to nanoparticles on the overall hydrogen production of the anaerobes. Moreover, the bio-char production was assessed along with the cost-benefit analysis of the integrated process.

2. Materials and Methods

2.1. Black liquor (BL) composition

The black liquor (BL) was harvested from paper making industry facility. The rice straw (RS) is the main source for manufacturing company which is abundant in Egypt. The RS was alkali pretreated by sodium hydroxide (1.75% w/v) at a temperature of 180 °C and pressure of 1.5 bars for 2 hrs. BL was brownish in color with a pH value exceeding 12.75 which was neutralized to

be 7.5 by phosphoric acid (77% conc.) to enrich the substrate with nutrients for bio-degradation processes. The BL contained suspended fibers in the bulk liquid and their characteristics are presented in **Table 1a.** The BL was mainly in a soluble form where the soluble COD (CODs) represented 98% of the total COD (CODt). The volatile solids to total solids (VS/TS) ratio were 0.5 due to the use of NaOH and H_3PO_4 for pre-treatment and neutralization of raw materials, respectively. The COD: N: P ratio of the BL was 12.3: 1: 3.2 and C/P ratio was 3.85. The total phenolic compounds (TPC) in the BL amounted to 1718±12.4 mg/L resulting a half maximal inhibitory concentration (IC_{50}) of 48.4±0.3 µg Gallic acid equivalent/ mL. Scanning electron microscope (SEM) and energy dispersive X-Ray (EDX) analysis were carried out for the BL **(Fig.1a and Table 1b**). The SEM image clearly showed the morphology of the dry crystals of the BL and the presence of fibers in the samples **(Fig. 1a).** Those fibers could be the remaining portions of lignin, cellulose and hemicellulose after alkali pre-treatment process. The oxygen and carbon represented 65% of the total weight of the elements (**Table 1b**). Sodium (Na) element percentage was quite high (26.59%) due to the alkali-pretreatment of rice straw. As expected the silica content was 5.2% and potassium (K) was 2.32%.

2.2.Mixed culture anaerobes

The anaerobes were collected from a full scale anaerobic digester located in Al-Gabal Al-Asfer, Cairo, Egypt. The sludge was dark black in color. The settleability of the inoculum sludge was quite high and amounted to 30 ml/gTS. The characteristics of the inoculum sludge are presented in **Table 1a.** The TS and VS contents were 132.04±0.34 and 72.75±035 g/l. The VS/TS ratio of the sludge was 0.55. The anaerobes were daily supplemented with BL for acclimatization period of 30 days. The CODs was quite low and represents 5% of the CODt. The CODp/CODt ratio was 0.95. The seed sludge was free from iso-butyrate (iso-HBu), propionate (HPr), formate (HFo) and acetate (HAc). α-amylase-, α- xylanase (used breach xylan), CM-cellulase (CM-cellulose) was 9.0±0.4, 400±7.8, 15±1.2 and 4.1±0.7 U/100 mL, respectively. SEM and EDX analysis were carried out for the inoculum sludge after adaptation process **(Fig. 1a)**. The morphology of sludge is compacted and flocculent free from granulation. The EDX analysis showed the sludge is rich of carbon (44.39%) and oxygen (30.96%). The sludge contained a percent of 5.12% for nitrogen, 3.19% for phosphorous, 2.36% for sulfur and 4.1% for calcium.

2.3.Preparation of solely and dual nanoparticles

Analytical grade chemicals were purchased from Sigma Aldrich for preparation of graphene oxide (nGO), graphene (nG), Magnetite (nM), graphene/magnetite (nG/M), hydroxyapatite (nHap) and graphene/hydroxyapatite (nG/Hap) at nano-scale. Preparation methods are explained in details in Supplementary data.

2.4. Experimental set-up

Anaerobic batch assays experiments were carried out in triplicate for a period of 14.0 days (350 hrs) (**Fig. 1b**). The serum bottles with a capacity of 300 ml were used for the experiments. The 1st bottles set was supplied with 100 ml sludge (S) (mixed culture anaerobes) and 150 mL dist. water. Those bottles were used as a control to assess the gas production from the sludge. The 2nd bottles set were supplied with 100 mL sludge (S) (7.2 gVS/100mL) and 150 mL black liquor (BL) (3.3 g CODt/150 mL) resulting in food to microorganism (F/M) ratio of 0.46 gCODt/gVS in the reaction medium. The main reaction bottles sets were inoculated with the following components i.e. 100 mL (S)+ 150 mL (BL) + 50 mg/gVS (nG); 100 mL (S)+ 150 mL (BL) + 50 mg/gVS (nGO); 100 mL (S)+ 150 mL (BL) + 50 mg/gVS (nM); 100 mL (S)+ 150 mL (BL) + 50 mg/gVS (nG/M), 100 mL (S)+ 150 mL (BL) + 50 mg/gVS (nHap) and 100 mL (S)+ 150 mL (BL) + 50 mg/gVS (nG/Hap). pH value of all bottles sets was adjusted to 7.5 using phosphoric acid to be utilized as a source of nutrient and suitable for growth of anaerobes. The batch bottles had a head space of 50 mL to allow the gas production. The bottles were flushed for 3 minutes using nitrogen gas to create anaerobic conditions in the reaction medium. The bottles set was incubated at a temperature of 35 ± 0.2 ºC. The volumetric gas production was daily measured along fermentation time of 350 hrs using a syringe method according to Owen et al., (1979). The biogas composition was daily measured and the hydrogen potential (P- mL), maximum hydrogen production rate ($R_{max.}$- mL /h) was simulated based on Gompertz equation model (**Eq. 1**),

$$H(t) = P * exp\left\{-exp\left(\frac{R_m * e}{P}\ (\lambda - t) + 1\right)\right\} \qquad Eq.1$$

Where H: is the cumulative H_2 production (mL), t: is the fermentation time (h) and λ: is the lag phase duration (h)

2.5. Pyrolysis process for bio-char production and net energy calculations

This experiment was conducted to fully utilize the black liquor (BL) providing a zero waste technology via bio-(H_2 & char) production. Duplicate samples (50 ml) of the digestate resulted from anaerobic digestion of sludge (S), black liquor (BL) and nG/Hap (50 mg/gVS) was placed in a porcelain dish and burnet at 550 °C for 1.0 h. The required energy for conversion of the digestate into bio-char followed the Auger-based pyrolysis system. Two steps are basically carried out for pyrolysis processes i.e. the reduction moister and digestate drying at an oxygen-free environment at 550 °C. Vapors released from the pyrolysis step are mainly recycled to maximize the drying step as well as operating the pyrolyzer (Campbell et al., 2018). Characterization and analysis of the bio-char were carried out for further reuse in agricultural purposes. Economic and cost benefit analysis of the combined process (fermentation/pyrolysis) was assessed. The energy consumption for anaerobic digestion process is mainly utilized for mixing and heating the digester. The following equation (**Eq. 2**) was used to calculate the energy consumption for heating the reactor up to 35 ºC.

$$E_H = C_p * M * dT\ /x \qquad Eq.2$$

Where, E_H: is the energy required for heating the reactor (kJ/l feedstock); C_p : is the specific heat constant (C_p of the water = 4.186 kJ/kg.K); M: is the weight of the sludge inside the batch reactor (kg),x: is the influent total solids and dT: is the difference between the initial (20 ºC) and operational temperature (35 ºC) (Perera et al., 2010). The energy consumed for mixing E_m was calculated based on the horse power of the mixer (0.05 HP) and operational time. Hydrogen energy E_{H2} (kJ/Lfeedstock) was estimated from **Eq. 3,**

$$E_{H2} = \ G * \rho_{H2} * LHV_{H2}/x \qquad Eq.3$$

Where, G :is the volume of hydrogen (L); $\boldsymbol{\rho}_{H2:}$ is the density of hydrogen gas (8.9×10^{-5} kg/L); and LHV is the lower heating value of hydrogen (120,000 kJ/kg) (Perera et al., 2010).

$$Net_{energy}(Kj/l)substrate = E_{H2} - E_H - E_M \quad Eq.4$$

The net energy was calculated from **Eq. 4** where hydrogen energy (EH_2), was subtracted from E_H and E_M. The electrical energy cost utilized for bio-char production was estimated by Huang et al., (2015) to be 43 $/feedstock for a small scale auger-based pyrolysis system.

2.6. Analytical methods

The black liquor (BL), sludge (S) and nanoparticles (N_p) were analyzed. The pH value was measured using JENWAY 3510. CODt, CODs, CODp, total solids (TS), volatile solids (VS), total phosphorous (TP), TKJ-N and NH_4-N were determined based on APHA, (2005). CODs was filtered using membrane filter (0.45 µm) and the CODp was calculated by the difference between CODt and filtered COD. Volatile fatty acids (VFAs) in terms of formate (HFo), propionate (HPr), iso-butyrate (HBu), acetate (HAc), valerate (HVa) were determined by High Performance Liquid Chromatography (HPLC).

Scanning electron microscopy (SEM) and energy dispersive X-Ray (EDX) was used to observe the morphology of the sludge and elemental analysis content. Transmission electron microscope TEM, Model JEM-2010, Japan, was used to investigate particle size and morphology. Fourier-transform infrared spectroscopy (FTIR) analysis was used to detect the presence of the main organic groups that constitute the BL, sludge and bio-char. FTIR analysis was carried out in the range of 450 to 4000 cm^{-1} using a Fourier Transform infrared spectrophotometer (JASCO 6100 spectrometer, Japan). X-Ray Diffraction (Schimadzu XRD 7000, Japan) was used for characterization of the BL and S samples.

Enzymatic assays of microbial carbohydrate-cleaving enzymes in terms of polygalacturonase, α-xylanase, CM-cellulase and α-amylase (EC3.2.1.1) activities were measured by determination of the liberated reducing end products using galacturonic acid, xylose, glucose and maltose, respectively as standards (Miller, 1959). One unit of enzyme activity was defined as the amount of enzyme which liberated 1 µmol of reducing sugar/h under standard assay conditions. The total phenolic content of the samples was measured by the method described earlier by Velioglu et al., (1998). The results are expressed as mg gallic acid equivalent (GAE)/ ml according to a gallic acid standard curve. The antioxidant activity of the samples was determined by (2, 2-azino-bis (3-ethylbenzo-thiazoline-6-sulfonic acid) (ABTS) based on the method of (RE et al., 1999) and **Eq. 5.** Carbohydrates were determined according to Dubois et al., (1956). Glucose served as the calibration standard for total carbohydrate determination. The reduction method of methylene

blue was used for measurement of hydrogenase enzyme activity (Lee et al., 2009). Protein content was determined as described by Emami Bistgani et al., (2017) using bovine serum albumin as standard.

$$ABTS\ scavenging\ ((\%) = \left\{\frac{O.D_{control} - O.D_{sample}}{O.D_{control}}\right\} X100 \quad Eq.5$$

2.7. Microbial community analysis

Samples from batch assays have been collected for DNA extraction, quantitative PCR and community analysis using Single Strand Conformation Polymorphism (SSCP) (methods in details in supplementary data). OTU assignments and statistical analysis was carried out based on the extracted DNA (see supplementary).

3. Results and discussion

3.1.Impact of supplementation of solely and dual nano-particles (nPs) on the efficiency of anaerobes treating black liquor

Characterization of solely and dual nano-particles (nPs) has been assessed using different parameters. X-ray diffraction, Fourier transform infra-red spectroscopy, scanning electron imaging and transmission electron microscopies have been applied to characterize the prepared nPs (characterization in details see supplementary data).

3.1.1.Hydrogen production (HP) and Yield (HY)

Nano-metals are playing a key role for hydrogen fermentative process i.e. iron (Fe) acts as serve factor for hydrogenase enzyme (HE) secretion and intercellular electron transfer. Addition of Fe (concentration of 18–55 mg/L) increased hydrogen yield (HY) by 1.5 fold and reduced the lag phase period by 0.33 fold (Kim et al., 2011). The efficiency of anaerobes for HP and HY were increased due to supply of calcium (Ca) concentration of 50–150 mg/L in the reaction medium (Chang and Lin, 2006). The hydrogen fermentative of BL was comprehensively investigated by immobilization of anaerobes on the solely and dual nano-particles (nPs) as shown in **Fig. 2a.** The experimental results were closely fitted to the simulated ones with R^2 ranging from 0.895 to 0.993. The hydrogen potential (P) and HY was quite low for the control batches containing only anaerobes and BL which was amounted to 198.5 ±10.8 mL and 44.6 ± 3.8 mL/gCODs $_{removed}$, respectively. Those values were significantly ($p< 0.05$) increased up to 274.0± 11.8 mL and 63.8

± 3.9 mL/gCODs $_{removed}$ when the anaerobes supplemented with 50 mg/gVS nG. This was mainly due to an increase of hydrogenase enzyme (HE) activity from 0.08±0.001 (control) to 0.108 ± 0.004 mg M.B reduced/min for anaerobes supplemented with 50 mg/gVS nG. The addition of nG facilitates the electron transfer between the substrate and anaerobes and plays a crucial role as a carrier for anaerobes creating unusual conditions for hydrogen producing bacteria (HPB). The surface area of nG is quite high to facilitate the electrons adsorption and subsequently electron transfer between nG and hydrogenase enzyme (HE) molecules to catalyze the conversion of H_2 to proton and vice versa. Moreover, the addition of nG increased the enzymatic activities degrading proteins and carbohydrates i.e. α-amylase, α- xylanase, CM-cellulase, and protease by values of 44.7±1.9, 93.9±1.2, 25.0±0.9, 100±6.35%, respectively. Likely HY and P was increased by values of 37.6 and 34.4% for anaerobes supplemented with 50 mg/gVS nGO where the HE activity was 0.117 ± 0.003 mg M.B reduced/min. The P and HY was better for anaerobes supplemented with 50 mg/gVS magnetite (nM) due to it is composed of iron which play a key role for enhancement of metabolism of hydrolytic bacteria and subsequently hydrogen production. The P values of nM exceeded by 47.5 and 123 mL as compared to nG and control samples respectively. Similar observation was recorded for HY where it was better by values of 38.4% and 44.9% as compared to anaerobes free nPs. The HY was further increased by 75.5 mL and 36.4 mLH_2/gCODs $_{removed}$, respectively. This was mainly due to the addition of magnetite (nM) which reduced the half maximal inhibitory concentration (IC_{50}) from 49.1±2.8 µg gallic acid equivalent/mL for BL to 15.75±2.5 µg gallic acid equivalent/mL for anaerobes supplemented with nM. Moreover, addition of magnetite to the reaction medium reduced the lag phase from 72 hrs for control to 36 h due to a high activity of HE (0.14 ± 0.003 mg M.B reduced/min). Likely, immobilization of anaerobes on Fe_2O_3 NPs Improved HY by 57.8% (0.90 mol H_2/mol glucose) from starch wastewater (Nasr et al., 2015). HY was increased by 26.4% (1.53 mol H_2/mol glucose) by anaerobic sludge supplemented with 400 mg/L of Fe_3O_4 NPs under mesophilic conditions (Zhao et al., 2011). However, 50 mg/L of Fe_3O_4 NPs was sufficient to increase the HY by value of 83.3% (44.3 l/kg COD) by mixed culture from distillery wastewater (Malik et al., 2014). Addition of 400 mg/L Fe-nPs to the mixed bacterial consortium fed with glucose caused a reduction of HY by 38% (1.23 mol/mol hexose) (Zhang et al., 2015). Incorporation of graphene (nG) with magnetite (nM) for immobilization of anaerobes highly increased the P and HY as shown in **Fig. 2a**. The P (211.5±10.2 mL) and HY (106 .3 ±2.7mL

H_2/gCODs $_{removed}$) were quite high and increased by value of 51.6 ± 2.1and 61.6±1.6% as compared to the control batch assay. A significant (P≤0.05) improvement of 24.03 % for P and 20.4% for HY was occurred due to the use of dual nano-particles (nG/M). This was mainly due to an increase of HE activity from 0.14±0.003 to 0.178±0.02 mg M.B reduced/min). Moreover, the enzymatic activities of α-amylase, α- xylanase, CM-cellulase, polygalacturonase and protease were increased by 59.0±2.5, 75.2±2.6, 10±0.9, 88.5± 4.7and 95.7±10.2%, respectively. The ABTS (Scavenging %) was increased from 31.9±2.9 to 89.2±0.6% with supplementation of 50 mg/gVS of nG/M onto the anaerobes. This indicates that the use of dual nanoparticles would increase the antioxidant activity and enhance the HY. Likely, Mostafa et al., (2016) found that supplementation of anaerobes with 100 mg/L magnetite/graphene oxide (MGO) increased the HY up to 112.4±10.5 $mLH_2/gCOD_{removed}$ from gelatinous wastewater and the conversion efficiency of carbohydrates, proteins and lipids was promoted up to 80.8±7.6, 34.4±2.3 and 31.4±2.2%, respectively. H_2 production was significantly increased by 1.2-1.5 times with anaerobes supplemented with hematite and nickel oxide NP as compared to control batches resulting an increase of HY by a value of 32.6% (Han et al., 2011).

The addition of calcium ions onto the anaerobes will maintain a high cell density in the digester and induce microbial aggregation (Kosaric et al., 1990). Moreover, Ca^{2+} would improve granulation process by facilitating early aggregation resulting large particle sizes and more biomass growth. The addition of Ca^{2+} to the anaerobic reactor improved sludge granulation by adsorption, adhesion and multiplication process (Chang and Lin, 2006). Moreover, the presence of Ca^{2+} would enhance the secretion of extracellular polymeric substance (EPS) to keep the ionic balance in the reaction medium. Moreover, EPS are playing a key role for cell binding and agglomerate the anaerobes due to electrostatic interaction force. EPS is always negatively charged and can easily bind with positively charged organic pollutants and facilitate the metabolism process of the organic content of the BL. EPS prefer to bind with divalent ions in the reaction medium to form of more stable complexes (Chang and Lin, 2006). Accordingly, the use of hydroxyapatite (nHap) rich with calcium and phosphorous ions in nano-scale was attempted here for enhancement of HP and HY from BL as shown in **Fig. 2a**. However, the P of 335±8.7 ml and HY of 71.7 ±4.7ml/gCODs $_{removed}$ were lower than those obtained from the dual nanoparticles of (nG/M). Yuan et al., (2010) found that supplementation of 100 mg/L calcium improved the cell retention, density by two-fold, hydrogen production rate (HPR) and HY of

24.5 L/d/L and 3.74 mol H_2/ mol sucrose, respectively. Calcium ion addition of 75 - 150 mg/L enhanced the granulation process and increased HY up to 3.6 mol H_2/mol-sucrose and HPR of 807 mmol-H_2/L-d. However, the HPR and HY were deteriorated at Ca concentration of 300 mg/L (Chang and Lin, 2006).

The dual nano-particles of nG/Hap was attempted to improve the P and HY as shown in **Fig. 2a.** The P and HY was maximized up to 514± 11.6 mL and 115.9±12.2 mL /gCODs $_{removed}$ at a dose of 50 mg/gVS. Those values are higher than those achieved by nG/M by values of 104 mL & 9.6 mL/gCODs $_{removed}$ and control samples by 61.3±4.1 and 61.5±2.3%, respectively. This was mainly due to the addition of nG/Hap which enhanced and improved the secretion of EPS from 222 ±11.3 to 248± 8.9 mg/gVS and HE from 0.178±0.02 to 0.28 ± 0.004mg M.B reduced/min as shown in **Fig. 2a.** Moreover, the lag phase period was largely reduced from 72 (control) to 12.0 h., and from 24 h (nG/M) to 12 h., (nG/Hap). This indicates that addition of nanoparticles rich calcium ions accelerated the biodegradation activities and subsequently HP and HY. Furthermore, the ABTS (Scavenging %) was increased from 31.9±2.9 to 89.9±0.28% due to the supplementation of nG/Hap. Likely, the HY was increased by 27% due to co-addition of NPs (50 mg/l Fe_2O_3 + 10 mg/l NiO) as compared with controls and a significant decrease of the lag phase from 3.6 to 2.8 h was occurred (Gadhe et al., 2015a). The HP of 150 l/kg VS was maximized at Fe and Ni concentration of 37.5 and 37.5 mg/L, respectively and the HY was improved by 200% as compared to controls (Gadhe et al., 2015b).

3.1.2. Enzymatic assays of microbial carbohydrate and protein -cleaving

Bacterial cells cannot directly up-take the macro-molecules i.e. carbohydrates and proteins present in BL. Therefore, anaerobes produce and/or excrete extracellular hydrolytic enzymes such as amylases, cellulases and proteases to breakdown and solubilize the macromolecular structures into simpler forms i.e. sugars and amino acids to facilitate transport of substrate through cell membrane (Mshandete et al., 2005). Those simple by-products are utilized by anaerobes to gain energy and synthesize new cellular components. Hydrolysis of cellulose is taken place by the cellulase enzyme to yield glucose while starch is converted into glucose by amylase enzymes (Parawira, 2012). Hydrolysis is the rate-limiting step of the anaerobic digestion process where, anaerobes degrade substrates containing high fractions of particulate organic matter. Fortunately, the major portions of organics in the BL were in the soluble form (98%).

Understanding of hydrolytic enzyme production, activities and its relations with nanoparticles supplementation are deeply discussed here. Enzymatic activities are the key of transformations of high molecular weight (HMW) organics into simple components to be easily utilized by anaerobes, i.e. conversion of proteins and carbohydrates into amino acids and glucose, respectively. Those metabolites are further converted by acidogenesis into volatile fatty acids (VFAs) and hydrogen gas. The BL contained a high protein and soluble carbohydrate content of 11.36±0.46 g/l and 43.5±12.7 g/l which needs to be hydrolyzed by anaerobes. Direct protein uptake by anaerobes is impossible and requires extracellular enzymes i.e. proteases to cleave HMW proteins into amino acids and peptides which can subsequently utilize and metabolize by acidogenesis into VFAs, sulfide, H_2 and ammonia (Tang et al., 2005). Likely, hydrolysis of carbohydrates needs particular enzymes i.e. α-amylase, α- xylanase, CM-cellulase and polygalacturonase for metabolism process. **Fig. 2b** shows the enzymatic activities of proteases, α-amylase, α- xylanase, CM-cellulase and polygalacturonase which was strongly dependent on the type of nano-particle (nPs) addition. The enzymatic activities of α-amylase, α- xylanase, CM-cellulase and protease was 31.5± 2.4, 4±0.2, 7.5±1.2 and 0 for control samples which was significantly ($P \leq 05$) increased up to 57± 2.1 and 69±2.3 U/100ml, 66.5±2.7 and 116±11.2 U/100ml, 10 ±0.2 and 14.5 ± 0.34 U/100ml, 335±11.7 and 155±4.3 U/100ml in the batches supplemented with nG and nGO, respectively **(Fig. 3a)**. Polygalacturonase activity was increased from 0 (nG) to 47.5±1.3 U/100ml for the samples containing nGO. This strongly indicates that the enzymes activities are promoted due to the supplementation of the anaerobes with nG and nGO. Amylase activity was quite high during mesophilic anaerobic digestion of solid potato waste compared to other hydrolases due to the existence of amylolytic microbes (Parawira, 2012). However, the enzymatic activities were significantly increased with the addition of dual nanoparticles i.e nG/M and nG/Hap as shown in **Fig. 3a**. The enzymatic activities of α-amylase, α- xylanase, CM-cellulase, polygalacturonase and protease were 57± 2.3, 66.5±4.3, 14.5±0.5, 59± 4.5, 165±8.7 and 112±11.2 U/100ml for anaerobes supplied with nG and increased up to 77±2.3, 131±3.2, 35±1.2, 291±12.5 and 740±23.7 U/100ml for nG/M. Supplementation of iron source into the reaction medium enhanced and promoted the enzymes activities, hydrolysis and subsequently the HY (**Fig. 3a**). Further promotion of enzymatic activities were occurred due to supplementation of graphene/hydroxyapatite (nG/Hap) where the α-amylase, α- xylanase, CM-cellulase, polygalacturonase and protease were increased by values of 52.5, 26.4, 32.7, 0.7 and

29.2 respectively. H_2 production was increased by 60–70% due to inoculation of digester with external hydrogen-producing bacteria with cellulolytic activity (*Caldicellulosyruptor saccharolyticus*) (Bagi et al., 2007). Feng et al., (2014) found that addition of 20 g/L Zero valent iron increased the activities of protease and cellulase up to 92.0 and 91.7%, respectively. Similar results were observed for extracellular polymeric substances (EPS) as shown in **Fig. 2a**. Hydrolytic enzymes i.e. cellulase and pronase E caused a reduction of 80% for solids and 93% removal of particulate COD (Roman et al., 2006) and the addition of α--amylase (0.06 g/g dry sludge) increased the hydrolysis rate constant from 0.106 to 0.215 h^{-1} and the activation energy for hydrolysis of volatile solids was reduced from 62.72 kJ/mol (control sample) to 20.19 kJ/mol (α -amylase treatment) (Luo et al., 2012). The EPS was 23 ±11 mg/gVS for fermented sludge and increased up to 78 ± 22 mg/gVS for fermentation of BL and sludge. Addition of substrate promoted the anaerobes to generate the EPS to enrich the reaction medium and agglomerate the bacterial cells for degradation of organics. Furthermore, the EPS generation was substantially enhanced due to enrich the anaerobes with solely and dual nano- particles (**Fig. 2a**). Better EPS generation was recorded based on the following order nG/Hap>nG/M>nM>nHap> nGO > nG. The maximum EPS generation of 248±30 mg/gVS was recorded for immobilization of anaerobes on the nG/Hap due to the presence of calcium ions. The presence of Ca ions increase the cell retention, and catalytic activity of anaerobes (Yu et al., 2002). Morgan et al., (1991) found that the addition calcium onto the anaerobes promotes extracellular polysaccharide constituents which utilized for cell bindings with the substrate. Addition of 150 mg-Ca^{+2}/L reactor provided the highest EPS values of the digester producing hydrogen from sucrose (Chang and Lin, 2006).

3.1.3. Proteins and carbohydrates conversion and ammonification process

The anaerobes supplemented with solely and dual nanoparticles provided a significant positive impact on the protein and carbohydrate degradation (**Fig. 3b**). The conversion of protein and carbohydrate was 1.0 and 1.22 g/l for control sample which was significantly increased up to 1.93 and 1.2 g/l for anaerobes supplemented with nM and to 2.7 and 1.5 g/l for nG/Hap samples. This can be attributed to a higher protease, α-amylase and α- xylanase activities and lower IC_{50} in the batches supplemented with nG/Hap. Likely, Feng et al., (2014) found that the degradation efficiency of proteins and carbohydrates was increased from 59.1 to 67.8% and from 32.3% to 43.4% using anaerobes immobilized on zero valent iron. Likely, the HY of 106.3±11.6

mL/gCODs $_{removed}$, 190±8.9 mL/g carbohydrate $_{removed}$, 339.4 ±13.9 mL H_2/g protein $_{removed}$ based on CODs, carbohydrate and protein conversion was quite high for anaerobes supplemented with nG/M and increased up to 115.9 ±12.6 mL/gCODs $_{removed}$, 190.6 ±9.8 mL/g carbohydrate $_{removed}$ and 365.4 ±14.3 mL H_2/g protein $_{removed}$ for nG/Hap. However, Yang et al., (2015) found that carbohydrate was more efficiently anaerobically biodegraded than protein resulting removal efficiencies of 49.7% and 32.2%, respectively.

Protease is essential enzyme for protein hydrolysis to form amino acids which subsequently metabolized to generate NH_4^+ in the reaction medium. The protease enzyme activities were quite high for anaerobes supplemented with nG/Hap which mitigated the known limiting step of protein decomposition. Accordingly, proteases enzyme activity is very important factor for ammonification. Ammonification process is occurred due to chemical reaction in which NH_2 groups are converted into ammonium (NH_4^+) and/or the N-org. is anaerobically converted into ammonia **(Eqs. 6 and 7).**

$$R - CH - NH_2 - COOH + HOH \rightarrow R - COOH + CO_2 + NH_4 \qquad Eq.6$$

$$CO\ (NH_2)_2 + HOH \rightarrow 2NH_3 + CO_2 \qquad Eq.7$$

The relationship between the ammonification process and protease enzyme activity are presented in **Fig. 3b** where the ammonification process was the optimum for anaerobes supplemented with nG/Hap. The ammonification process was optimized in the batches supplemented with dual nanoparticles i.e. nG/M and nG/Hap where, ammonia was increased in the reaction medium by values of -17% and -18%, respectively. These values were higher than those obtained for solely nanoparticles i.e. -2.4%, -5.5%, -10.5 and -11% for the anaerobes supplied with nG, nGO, nM and nHap, respectively. This was mainly due to the conversion of nitrogen (TKj-N) was quite high for the batches containing dual nanoparticles. TKj-N removal efficiency was 17.2% for nG, 25.3% for nGO, 26.5% for nM, 28.8% for nHap which was significantly increased up to 33.5% for nG/M and 34.7% for nG/Hap as shown in **Fig. 3b.**

3.1.4. Metabolite by-products

The acidogenesis process is employed for biodegradation of amino acids and sugars into volatile fatty acids (VFAs), H_2, H_2S and ammonia (NH_4-N). The acidogenesis process of BL was accompanied by dropping in the pH value of the reaction medium due to the production of

acetate (HAc), Iso-butyrate (Iso-HBu) and Valerate (HVa). The pH for all samples was dropped from 7.5±0.2 to the minimum value of 6.8 ±0.2 in case of the batches supplemented with solely and dual-nanoparticles. Theoretically, conversion of organics into HAc and HBu produces 4 and 2 mol of H_2 respectively (**Eqs. 8 and 9**). Production of propionate (Hpr) would consume the H_2 gas which should be avoided (**Eq. 10**) (Yuan et al., 2008). Acetate fermentation pathway is prevailed at HAc to HBu ratio > 1 (**Eq. 8**) and HAc/HBu < 1 provides butyrate fermentation pathway (**Eq. 9**).

$$\textbf{\textit{Acetate Pathway}}: C_6H_{12}O_6 + 2H_2O \rightarrow 2CH_3COOH + 2CO_2 + 4H_2 \quad Eq.8$$

$$\textbf{\textit{Butyrate pathway}}: C_6H_{12}O_6 \rightarrow CH_3CH_2CH_2COOH + 2CO_2 + 2H_2 \quad Eq.9$$

$$C_6H_{12}O_6 + 2H_2 \rightarrow 2CH_3CH_2COOH + 2H_2O \quad Eq.10$$

The results in **Fig. 3c** show the impact of supplementation of solely and dual – nanoparticles on the VFAs production in terms of valerate (HVa), iso-butyrate (iso-HBu), propionate (HPr), formate (HFo) and acetate (HAc) in the reaction medium. The fermentation of the inoculum sludge (S) was carried out as a control where, iso-butyrate (iso-HBu), propionate (HPr), formate (HFo) and acetate (HAc) was increased in the reaction medium up to 38.6±2.6 mg/L, 21.4 ±0.1 mg/L, 21.3±7.9 mg/L and 19.9±0.1 mg/L, respectively. The HVa, iso-HBu, HPr, HFo and HAc was 320 ±21 mg/L, 1244±100 mg/L, 267±12.9 mg/L, 344±10.9 mg/L and 653 ±22.8 mg/L in the control sample which was significantly increased up to 1026±123, 1628.6±78, 288.1±11.9, 927.8±8.8 and 1465.3±11.9 for nG and to 331±11, 1261±66,344±10.9, 340±9.8 and 733±10.8 mg/L for nGO. The H_2 production was low in the control samples due to the propionate (HPr) production in the reaction medium which consume the hydrogen and converted into acetate. The HY and HP were higher in the samples rich with nG and nGO than those achieved for control samples due to a higher production of HAc and Iso-HBu. However, butyrate fermentation pathway was dominant for the control, nG and nGO where the HAc/Iso-HBu ratio was 0.52, 0.9 and 0.58 respectively. Engliman et al., (2017) found that the HAc was maximized at a level of 32 mM at increasing iron NPs concentrations from 0 to 500 mg/L and acetate fermentation pathway was the major degradation mechanism. Moreover, the metal NP concentration was not consumed by the anaerobes and remained unaffected after the fermentation period. 200 mg Fe_2O_3 NP/L achieved maximum acetic acid of 13.57 mM and butyric acid of 31.21 mM from hydrogen

fermentative of complex distillery wastewater as a substrate (Gadhe et al., 2015b). HAc and HBu concentrations was significantly increased with the addition of hematite nanoparticles to the anaerobes compared with the corresponding control test (Han et al., 2011). Acetate (HAc) fermentation pathway was dominant for the samples supplemented with nM and nHap where the HAc was 344.3 ±89 and 2005.2 ±10.2 mg/L, respectively and the iso-HBu was absent in the digestate. However, the HPr production was quite high and amounted to 1294.9±11.9 and 1547.7±11.9 mg/L in the reaction medium resulting in a drop in the HY and HP. The HP and HY was quite high for the samples containing dual nanoparticles i.e. nG/M and nG/Hap due to the dominance of acetate fermentation pathway and lower production of HPr in the digestate. The HVa, iso-HBu, HPr, HFo and HAc was 388±89, 1514±56, 276±12.9, 367±11 and 1812±16.2 mg/L in the digestate of the sample containing nG/M with HAc/iso-But ratio of 1.2. Iso-butyrate was absent in the samples containing nG/Hap indicating the acetate fermentation pathway resulting residual values of 1241±211 mg/L for HVa, 1042.8±11.2 mg/L for HPr, 107.2±9.8 mg/L for HFo and 527.3±11.8 mg/L in the digestate. Co-addition of NiO NP, the Fe_2O_3 NP provided the maximum production of 39.60 mM for butyric acid and 15.23 mM for acetic acid from anaerobic digestion of complex distillery wastewater (Gadhe et al., 2015b). HAc concentration was significantly increased from 705.31 ± 56.20 to 1229.22 ± 86.47 mg/L in the bulk liquid of anaerobic fermentation of petrochemical wastewater industry at increasing the dosage of nNi/G from 0 to 60 mg/L respectively (Elreedy et al., 2017).

3.1.5.Total phenolic compounds (TPC), total reducing sugars (TRS), the half maximal inhibitory concentration (IC_{50} -µg gallic acid equivalent/mL) and antioxidant activity –ABST Scavenging %)

The BL contains total reducing sugars (TRS) of 262.8±11.9 mg/L which are mainly glucose and fructose fractions. Those mono-saccharides are further biodegraded by acidogenesis process as shown in **Fig. 3d** and reported earlier by (Zeng et al., 2017). The results showed that the TRS removal was increased in the samples supplemented with solely and dual-nanoparticles. The TRS removal efficiency was maximized at levels of 65.4 ±1.2and 68.2±1.3 % for the anaerobes supplemented with nG/M and nG/Hap respectively. Antioxidants could be natural phenolic compounds (tocopherols, flavonoids, and phenolic acids), nitrogen compounds (alkaloids, chlorophyll derivatives, amino acids, and amines), or carotenoids as well as ascorbic acid

(Velioglu et al., 1998). The polyphenols are very strong antioxidant compounds causing de-oxygenation of the waters (El Moudden et al., 2019). The results in **Fig. 3d** clearly show the relationship between the antioxidant activities ABTS-scavenging %) and the total phenolic compounds (TPC) content. The antioxidant activity ABTS-scavenging (%) was increased from 31.9±2.9 (initial) to 89.2± 0.6 for nG/M and to 89.8±0.3 for nG/Hap. This was mainly due to a drop of TPC from 171.8 ±12.4 mg/100mL (initial) to 90.5 ±20.5 mg/100mL for nG/M and to 93±2.8 mg/100mL for nG/Hap (**Fig. 3d**). Apparently, immobilization of anaerobes on the dual – nanoparticles mitigated the inhibition effect of TPC and increased the antioxidant activity which subsequently enhanced the HY and HP. Likely, El Moudden et al., (2019) found that the antioxidant activity and phenolic compounds are inversely proportional relationship. The removal efficiencies of TPC were 36.3±0.3% for nG, 38.3±0.7% for nGO, 38.9±0.9% for nM and 43 ±1.2% for nHap. Those values were slightly increased for dual nano-particles i.e. 47.3±1% for nG/M and 45.9±1.2% for nG/Hap. Likely, Hernandez and Edyvean, (2008) achieved the maximum biodegradation of phenolic compound of 63.85±2.73%, by anaerobes. However, the inhibition of methanization was occurred at high influent phenolic compounds of 800 and 1600 mgTPC/L.

The black liquor (BL) contains phenolic compounds of 171.8±12.4 mg/l00mL which resulted from chemical pulping of agriculture waste components. The presence of phenolic compounds in the substrate would inhibit the anaerobes and subsequently decrease the H_2 generation where the half maximal inhibitory concentration IC_{50} *(*µg gallic acid equivalent/mL*)* was accounted for 49.1±2.8 µg gallic acid equivalent/mL for initial substrate (**Fig. 3d**). The IC_{50} was significantly dropped to 16.4 ±1.1 µg gallic acid equivalent/mL due to immobilization of anaerobes on the nG and the total phenolic compounds were removed by value of 36.2±0.3 %. Moreover, the IC_{50} was further decreased up to 15.7 ±2.5 µg gallic acid equivalent/mL for anaerobes supplemented with nM due to the removal of phenolic compounds (38.9±0.9%). IC_{50} was minimum i.e. 14.7 ±0.6 and 13.1 ±2.7 µg gallic acid equivalent/mL for dual nanoparticles (nG/M and nG/Hap) respectively. This indicates that supplying of solely and dual nano-particles onto the anaerobes degrading BL substantially promotes the antioxidant and enzymatic activities, reduces the inhibition IC_{50} effect of the phenolic compounds and surprisingly enhanced the hydrogen yield and production.

3.2. Microbial community

3.2.1. Bacterial α-diversity and community structure

A total number of 145,551 effective sequences were obtained for anaerobes supplemented with nG/Hap, nG/M, nM, and nHap (ranging from 30,881 to 39,873 across all samples). As shown in **Figs. 4a-b**, the anaerobes supplemented with nG/Hap displayed the highest species richness compared to the other samples, while those supplemented with nHap showed the lowest ACE and Chao1. Meanwhile, we observed higher species evenness in the anaerobes exposed to dual nano-particles (nG/Hap and nG/M) as compared to solely nano-particles (nM and nHap) based on the Simpson and Shannon indices (**Figs. 4c-d**). Such results indicated that the dual nano-particles increased the biodiversity of the anaerobes where specific bacteria became dominate in the population immobilized on dual nanoparticles (N1) and disappeared with solely nanoparticles i.e. nHap and nM (N3 and N4). Previous study demonstrates that biodiversity acts as the insurance of community productivity (Awasthi et al., 2014) which may be the reason why anaerobes immobilized on dual nanoparticles enjoyed the highest HY.

The results in **Fig. 4e** show the taxanomy of the samples harvested from batches containing nG/Hap, nG/M, nM and nHap (N1,N2,N3 and N4) to assess the variations of consortium and its relation with the biodegradation process. Data displayed that all samples (N1,N2,N3 and N4) were dominated by the phyla *Proteobacteria* (average 34.53%), *Firmicutes* (average 27.55%), *Chloroflexi* (average 10.19%), *Actinobacteria* (average 9.44%), *Planctomycetes* (average 6.64%), *and Bacteroidetes* (average 3.82%). Therein, the relative abundances of *Proteobacteria* and *Actinobacteria* were relatively lower in the anaerobes immobilized on dual nanoparticles (N1 and N2) than those on solely nHap and nM (N3 and N4). In contrast, the addition of solely nanoparticles was found to increase the abundances of *Chloroflexi* and *Bacteroidetes*. However, no substantial difference was found in the common hydrogen producers, i.e., *Firmicutes*, between the sludge immobilized on dual and solely nanoparticles.

3.2.2. Network analysis

The bacterial interaction network of anaerobes is illustrated in **Fig. 5**. The network consisted of 13 modules, which largely varied in size and shape. The largest module contained 56 species, while only one specie is detected in the smallest modules. Meanwhile, the topological roles analysis (**Fig. 5b**) showed that only 7.0 OTUs were peripherals, while the remaining 127 OTUs

were the connectors. No module or network hub was identified. Such result suggested the blurring boundaries among the modules and the effects of external perturbations on one OTUs can spread to the other OTUs in the network (Olesen et al., 2007). As such, the responses of community members to nanoparticles exposure should affect the hydrogen producers. As shown in **Fig. 5c**, the *Firmicutes* were more likely to negatively correlate with the *Actinobacteria*. With regard to the *Bacteroidetes* and *Chloroflexi*, they were more likely to co-occur with the *Firmicutes*. Moreover, we observed the same numbers of positive and negative edges between *Firmicutes* and *Proteobacteria*, suggesting that the latter can either promote or inhibit the hydrogen producers. Upon exposure to dual nanoparticles, the *Actinobacteria* were inhibited but more *Bacteroidetes* and *Chloroflexi* were observed as compared to those immobilized on solely nanoparticles. Therefore, it is expected that the dual nanoparticles can neutralize the competition and promote the metabolic cooperation in community for *Firmicutes*, and thus increased the HY.

3.3. Bio-char production, net gain energy and profits

The digestate resulted from fermentation of S+BL+ nG/Hap was burnt at temperature of 550 ºC to harvest the bio-char. The proportions of carbon (C), nitrogen (N), oxygen (O), phosphorus (p) and potassium (K) and micro-nutrients was characterized by diffractometry of X- rays; functional groups by infrared absorption spectroscopy (FTIR) and scanning electronic microscope (SEM) (**Fig. 6a) and Table 2**. The results showed that the bio-char contained 13.73% for C, 11.98% for Na, 1.72% for K and 6.48% for P. The O/C ratio of 2.73 was quite low indicating a high degree of condensation and structures with aromatic rings which are responsible for chemical stability of the biochar, thus increasing resistance to microbial degradation in the soil (Ma et al., 2016). The SEM analysis showed that the bio-char was mainly white/grey in color and had a surface area of 2.4 ± 0.95 m^2/g, density of 1.63 ± 0.18 g/cm^3, pore volume of 0.2 ± 0.06 cm^3/g. The bio-char yield was 33±5.2%.

Diffractometry of X- rays of the resulted bio-char are presented in **Fig. 6c** where a peaks of kaolinite (7.14, 3.58, 2.34 Å), quartz (3.33, 4.27, 2.28, and 1.82 Å), and hematite (1.44 and 1.83 Å) were detected. Moreover, a peaks characteristic of goethite (3.38, 4.20, 2.45, 2.14 Å) and calcite (3.80, 2.28, and 2.10 Å), were observed. The CI of the bio-char was 27.7%. Sharp peaks in the sample indicated the presence of various inorganic elements such as silica (Si), which are mainly related to the crystalline forms of bio-char (Shaaban et al., 2013). Four broad peaks were

observed at the 2θ value of 9°, 26.713°, 34.136° and 35.073°. The peaks at 2θ (20.78°,26.713°, 27.75°, 31.80°) referred to the stacking structure of aromatic layers i.e. graphite 002 which originated from the small dimensions of crystallites perpendicular to aromatic layers (Omara et al., 2020). Moreover, a sharp, non-labeled peaks presented in the bio-char indicating miscellaneous of inorganic components (Si, P,K,Mg). The sharp and the strongest peak at 2θ of 26.713° is mainly originated from crystalline SiO_2 and confirmed heterogeneous surface of bio-char (Liu et al., 2012).

Carbonization process could increase aromatic structures and polymerization of the resulted bio-char. However, only five peaks were observed at wavenumbers of 3449.45, 1635.31, 1045.67, 571.05 and 458.19 cm^{-1} (**Fig. 6b**). A peak was observed at wave length number of 3449.45 cm^{-1} for compounds containing O-H group where hydrogen bonded -OH is stretched due to the presence of phenolic compounds (Shaaban et al., 2013). A small peak was detected at wave length number of 1635.31 cm^{-1} due to the presence of amide group and C=C of the Cis-unsaturated alkenes. A big and sharp peak was detected at 1045.67 cm^{-1} for C-O bonds indicating the presence of the alcohol and ester group. The vibrations of the aromatic groups were occurred at frequency of 571.05 and 458.19 cm^{-1} **(Fig. 6b).** A sharp peak at 458.19 cm-1 indicated the presence of silica in the bio-char which confirmed by the results of EDX and XRD analysis.

The net energy and profits gained from hydrogen fermentative and bio-char production from black liquor (BL) was briefly assessed. The energy consumption for hydrogen production (E_{H2}) form BL was accounted for 2.75 Kj/d. The calculated net energy gain from hydrogen production is 5.5 Kj/L based on the maximum hydrogen production of 514.5 mL. The calculated energy consumption for mixing was 0.7 Kj/L and the calculated net energy gain was 2.04 Kj/L BL which equivalent to 1.10 $/L feedstock. Those values are higher than those obtained by Soltan et al., (2019) where the net energy gains were 1.09 kJ/gfeed-stock from hydrogen fermentative of 50% pea + 50% banana. The profits from bio-char should be added to evaluate the total energy gained from the fermentation and pyrolysis process. Bio-char price varied from 0.09 to 8.85 $/kg (Opatokun et al., 2016). Accordingly the total profit from hydrogen fermentative and bio-char production is calculated to be 3.0 $/L. A higher gain profits were recorded by Soltan et al., (2019) where the combination of fermentation and pyrolysis processes of vegetables and fruits peels provided 5.21 $/kg feedstock.

4. Conclusions

Hydrogen fermentation of black liquor (BL) is a promising approach from economic and environmental point of view. Immobilization of solely and dual nanoparticles on anaerobes enhanced the HY and mitigate the inhibition effect of phenolic compounds. The dual nano-particles of nG/Hap provided P and HY of 514± 11.6 mL and 115.9±12.2 mL /gCODs $_{removed}$ which are higher than those achieved by nG/M by values of 104 mL & 9.6 mL/gCODs $_{removed}$ and control samples by 61.3±4.1 and 61.5±2.3% respectively. This was mainly due to an increase of EPS from 222 ±11.3 to 248± 8.9 mg/gVS and HE from 0.178±0.02 to 0.28 ± 0.004mg M.B reduced/min for nG/M and nG/Hap respectively. The HY was maximized for anaerobes supplemented with nG/M and nG/Hap due to the dominant of acetate fermentation pathway where the HAc was 344.3 ±8.9 and 2005.2 ±10.2 mg/L respectively and the iso-But was absent in the digestate. The phosphorous and calcium was detected in the digestate after fermentation period of 14 days which indicates that the nG/Hap was not consumed by anaerobes and played a key role for catalytic activity of microbes. The bio-char contained 13.73% for C, 11.98% for Na, 1.72% for K and 6.48% for P. The O/C ratio of 2.73 was quite low indicating a high degree of condensation and structures with aromatic rings which are responsible for chemical stability of the bio-char, thus increasing resistance to microbial degradation in the soil.

Acknowledgements

The authors are very grateful to Science Technology Development Fund (STDF) (Project ID: 26271, 41591), Academy of scientific research and technology (ASRT) (Code: Call no. 2/2019/ASRT-Nexus) and Imhotep project for partially financially support the research. The last author is grateful for the National Research Centre for partially supporting the research (Project ID: 12030202). This study was partially funded by the National Key R&D Program of China (No. 2017YFE0114300)

References

Andersson, E., Harvey, S., 2006. System analysis of hydrogen production from gasified black liquor. Energy 31, 3426–3434. https://doi.org/10.1016/j.energy.2006.03.015

APHA, 2005. Standard Methods for the Examination of Water and Wastewater. 25th ed. Washington, DC Am. Public Heal. Assoc. Water Work. Assoc. Water Environ. Fed.

Awasthi, A., Singh, M., Soni, S.K., Singh, R., Kalra, A., 2014. Biodiversity acts as insurance of productivity of bacterial communities under abiotic perturbations. ISME J. 8, 2445–2452. https://doi.org/10.1038/ismej.2014.91

Bagi, Z., Ács, N., Bálint, B., Horváth, L., Dobó, K., Perei, K.R., Rákhely, G., Kovács, K.L., 2007. Biotechnological intensification of biogas production. Appl. Microbiol. Biotechnol. 76, 473–482. https://doi.org/10.1007/s00253-007-1009-6

Bharath, G., Ponpandian, N., 2015. Hydroxyapatite nanoparticles on dendritic α-Fe2O3 hierarchical architectures for a heterogeneous photocatalyst and adsorption of Pb(II) ions from industrial wastewater. RSC Adv. 5, 84685–84693. https://doi.org/10.1039/c5ra15703j

Campbell, R.M., Anderson, N.M., Daugaard, D.E., Naughton, H.T., 2018. Financial viability of biofuel and biochar production from forest biomass in the face of market price volatility and uncertainty. Appl. Energy 230, 330–343. https://doi.org/10.1016/j.apenergy.2018.08.085

Chang, F.Y., Lin, C.Y., 2006. Calcium effect on fermentative hydrogen production in an anaerobic up-flow sludge blanket system. Water Sci. Technol. 54, 105–112. https://doi.org/10.2166/wst.2006.867

Darmawan, A., Ajiwibowo, M.W., Biddinika, M.K., Tokimatsu, K., Aziz, M., 2019. Black liquor-based hydrogen and power co-production: Combination of supercritical water gasification and syngas chemical looping. Appl. Energy 252, 113446. https://doi.org/10.1016/j.apenergy.2019.113446

Dubois, M., Gilles, K.A., Hamilton, J.K., Rebers, P.A., Smith, F., 1956. Colorimetric Method for Determination of Sugars and Related Substances 350–356.

El Moudden, H., El Idrissi, Y., El Yadini, A., Harhar, H., Tabyaoui, B., Tabyaoui, M., 2019. Effect of filtration of olive mill wastewater on the phenolic composition and its influence on antioxidant activity. Pharmacologyonline 2, 161–176.

Elreedy, A., Fujii, M., Koyama, M., Nakasaki, K., Tawfik, A., 2019. Enhanced fermentative hydrogen production from industrial wastewater using mixed culture bacteria incorporated with iron, nickel, and zinc-based nanoparticles. Water Res. 151, 349–361. https://doi.org/10.1016/j.watres.2018.12.043

Elreedy, A., Ibrahim, E., Hassan, N., El-Dissouky, A., Fujii, M., Yoshimura, C., Tawfik, A., 2017. Nickel-graphene nanocomposite as a novel supplement for enhancement of biohydrogen production from industrial wastewater containing mono-ethylene glycol. Energy Convers. Manag. 140. https://doi.org/10.1016/j.enconman.2017.02.080

Emami Bistgani, Z., Siadat, S.A., Bakhshandeh, A., Ghasemi Pirbalouti, A., Hashemi, M., 2017. Interactive effects of drought stress and chitosan application on physiological characteristics and essential oil yield of Thymus daenensis Celak. Crop J. 5, 407–415. https://doi.org/10.1016/j.cj.2017.04.003

Engliman, N.S., Abdul, P.M., Wu, S.Y., Jahim, J.M., 2017. Influence of iron (II) oxide nanoparticle on biohydrogen production in thermophilic mixed fermentation. Int. J. Hydrogen Energy 42, 27482–27493. https://doi.org/10.1016/j.ijhydene.2017.05.224

Feng, Y., Zhang, Y., Quan, X., Chen, S., 2014. Enhanced anaerobic digestion of waste activated sludge digestion by the addition of zero valent iron. Water Res. 52, 242–250. https://doi.org/10.1016/j.watres.2013.10.072

Gadhe, A., Sonawane, S.S., Varma, M.N., 2015a. Enhancement effect of hematite and nickel nanoparticles on biohydrogen production from dairy wastewater. Int. J. Hydrogen Energy 40, 4502–4511. https://doi.org/10.1016/j.ijhydene.2015.02.046

Gadhe, A., Sonawane, S.S., Varma, M.N., 2015b. Influence of nickel and hematite nanoparticle powder on the production of biohydrogen from complex distillery wastewater in batch fermentation. Int. J. Hydrogen Energy 40, 10734–10743. https://doi.org/10.1016/j.ijhydene.2015.05.198

Han, H., Cui, M., Wei, L., Yang, H., Shen, J., 2011. Enhancement effect of hematite nanoparticles on fermentative hydrogen production. Bioresour. Technol. 102, 7903–7909. https://doi.org/10.1016/j.biortech.2011.05.089

Hassan, M.A., Mohammad, A.M., Salaheldin, T.A., El-anadouli, B.E., 2018. A promising hydroxyapatite / graphene hybrid nanocomposite for methylene blue dye ' s removal in wastewater treatment 13, 8222–8240. https://doi.org/10.20964/2018.08.77

Hernandez, J.E., Edyvean, R.G.J., 2008. Inhibition of biogas production and biodegradability by substituted phenolic compounds in anaerobic sludge. J. Hazard. Mater. 160, 20–28. https://doi.org/10.1016/j.jhazmat.2008.02.075

Huang, Y., Anderson, M., McIlveen-Wright, D., Lyons, G.A., McRoberts, W.C., Wang, Y.D., Roskilly, A.P., Hewitt, N.J., 2015. Biochar and renewable energy generation from poultry litter waste: A technical and economic analysis based on computational simulations. Appl. Energy 160, 656–663. https://doi.org/10.1016/j.apenergy.2015.01.029

Jayabalan, T., Manickam, M., Naina Mohamed, S., 2020. NiCo2O4-graphene nanocomposites in sugar industry wastewater fed microbial electrolysis cell for enhanced biohydrogen production. Renew. Energy 154, 1144–1152. https://doi.org/10.1016/j.renene.2020.03.071

Kahrizi, P., Mohseni-Shahri, F.S., Moeinpour, F., 2018. Adsorptive removal of cadmium from aqueous solutions using NiFe2O4/hydroxyapatite/graphene quantum dots as a novel nano-adsorbent. J. Nanostructure Chem. 8, 441–452. https://doi.org/10.1007/s40097-018-0284-3

Kevlich, N.S., Shofner, M.L., Nair, S., 2017. Membranes for Kraft black liquor concentration and chemical recovery: Current progress, challenges, and opportunities. Sep. Sci. Technol. 52, 1070–1094. https://doi.org/10.1080/01496395.2017.1279180

Kim, D.H., Kim, S.H., Kim, H.W., Kim, M.S., Shin, H.S., 2011. Sewage sludge addition to food waste synergistically enhances hydrogen fermentation performance. Bioresour. Technol. 102, 8501–8506. https://doi.org/10.1016/j.biortech.2011.04.089

Ko, C.H., Hsieh, P.H., Chang, M.W., Chern, J.M., Chiang, S.M., Tzeng, C.J., 2009. Kinetics of pulp mill effluent treatment by ozone-based processes. J. Hazard. Mater. 168, 875–881.

https://doi.org/10.1016/j.jhazmat.2009.02.111

Kortekaas, S., Field, J.I.M.A., 1998. Anaerobic-Aerobic Treatment of Toxic Pulping Black Liquor with Upfront Effluent Recirculation 86, 97–110.

Kosaric, N., Blaszczyk, R., Orphan, L., 1990. Factors influencing formation and maintenance of granules in anaerobic sludge blanket reactors (UASBR). Water Sci. Technol. 22, 275–282. https://doi.org/10.2166/wst.1990.0092

Ksibi, M., Amor, S. Ben, Cherif, S., Elaloui, E., Houas, A., Elaloui, M., 2003. Photodegradation of lignin from black liquor using a UV/TiO2 system. J. Photochem. Photobiol. A Chem. 154, 211–218. https://doi.org/10.1016/S1010-6030(02)00316-7

Lee, D., Li, Y., Oh, Y., Kim, M., Noike, T., 2009. Effect of iron concentration on continuous H 2 production using membrane bioreactor. Int. J. Hydrogen Energy 34, 1244–1252. https://doi.org/10.1016/j.ijhydene.2008.11.093

Liu, Y., Zhao, X., Li, J., Ma, D., Han, R., 2012. Characterization of bio-char from pyrolysis of wheat straw and its evaluation on methylene blue adsorption. Desalin. Water Treat. 46, 115–123. https://doi.org/10.1080/19443994.2012.677408

Luo, K., Yang, Q., Li, X. ming, Yang, G. jing, Liu, Y., Wang, D. bo, Zheng, W., Zeng, G. ming, 2012. Hydrolysis kinetics in anaerobic digestion of waste activated sludge enhanced by α-amylase. Biochem. Eng. J. 62, 17–21. https://doi.org/10.1016/j.bej.2011.12.009

Ma, X., Zhou, B., Budai, A., Jeng, A., Hao, X., Wei, D., Zhang, Y., Rasse, D., 2016. Study of Biochar Properties by Scanning Electron Microscope – Energy Dispersive X-Ray Spectroscopy (SEM-EDX). Commun. Soil Sci. Plant Anal. 47, 593–601. https://doi.org/10.1080/00103624.2016.1146742

Malik, S.N., Pugalenthi, V., Vaidya, A.N., Ghosh, P.C., 2014. Kinetics of nano-catalysed dark fermentative hydrogen production from distillery wastewater. Energy Procedia 54, 417–430. https://doi.org/10.1016/j.egypro.2014.07.284

Miao, L., Li, F., Wen, J., 2009. Biological treatment of high-pH and high-concentration black liquor of cotton pulp by an immediate aerobic-anaerobic-aerobic process. Water Sci.

Technol. 60, 3275–3284. https://doi.org/10.2166/wst.2009.737

Miller, G.L., 1959. Use of Dinitrosalicylic Acid Reagent for Determination of Reducing Sugar. Anal. Chem. 31, 426–428. https://doi.org/10.1021/ac60147a030

Miranda, R., Negro, C., Blanco, A., 2009. Internal treatment of process waters in paper production by dissolved air flotation with newly developed chemicals. 1. Laboratory tests. Ind. Eng. Chem. Res. 48, 2199–2205. https://doi.org/10.1021/ie801047h

Morales, G., Pesante, S., Vidal, G., 2015. Effects of black liquor shocks on activated sludge treatment of bleached kraft pulp mill wastewater. J. Environ. Sci. Heal. - Part A Toxic/Hazardous Subst. Environ. Eng. 50, 639–645. https://doi.org/10.1080/10934529.2015.994974

Morgan, J.W., Evison, L.M., Forster, C.F., 1991. Changes to the microbial ecology in anaerobic digesters treating ice cream wastewater during start-up. Water Res. 25, 639–653. https://doi.org/10.1016/0043-1354(91)90039-S

Mostafa, A., El-Dissouky, A., Fawzy, A., Farghaly, A., Peu, P., Dabert, P., Le Roux, S., Tawfik, A., 2016. Magnetite/graphene oxide nano-composite for enhancement of hydrogen production from gelatinaceous wastewater. Bioresour. Technol. 216. https://doi.org/10.1016/j.biortech.2016.05.072

Mshandete, A., Björnsson, L., Kivaisi, A.K., Rubindamayugi, S.T., Mattiasson, B., 2005. Enhancement of anaerobic batch digestion of sisal pulp waste by mesophilic aerobic pre-treatment. Water Res. 39, 1569–1575. https://doi.org/10.1016/j.watres.2004.11.037

Nasr, M., Tawfik, A., Ookawara, S., Suzuki, M., Kumari, S., Bux, F., 2015. Continuous biohydrogen production from starch wastewater via sequential dark-photo fermentation with emphasize on maghemite nanoparticles. J. Ind. Eng. Chem. 21. https://doi.org/10.1016/j.jiec.2014.03.011

Nong, G., Zhou, Z., Wang, S., 2016. Generation of hydrogen, lignin and sodium hydroxide from pulping black liquor by electrolysis. Energies 9. https://doi.org/10.3390/en9010013

Olesen, J.M., Bascompte, J., Dupont, Y.L., Jordano, P., 2007. VR_Teenart177.pdf.

https://doi.org/10.1073/pnas.0706375104

Omara, H., Abdeelaal, G.M., Nadaoka, K., Tawfik, A., 2020. Developing empirical formulas for assessing the scour of vertical and inclined piers. Mar. Georesources Geotechnol. 38. https://doi.org/10.1080/1064119X.2018.1559901

Opatokun, S.A., Kan, T., Al Shoaibi, A., Srinivasakannan, C., Strezov, V., 2016. Characterization of Food Waste and Its Digestate as Feedstock for Thermochemical Processing. Energy and Fuels 30, 1589–1597. https://doi.org/10.1021/acs.energyfuels.5b02183

Owen, W.F., Stuckey, D.C., Healy, J.B., Young, L.Y., McCarty, P.L., 1979. Bioassay for monitoring biochemical methane potential and anaerobic toxicity. Water Res. 13, 485–492. https://doi.org/10.1016/0043-1354(79)90043-5

Parawira, W., 2012. Enzyme research and applications in biotechnological intensification of biogas production. Crit. Rev. Biotechnol. 32, 172–186. https://doi.org/10.3109/07388551.2011.595384

Perera, K.R.J., Ketheesan, B., Gadhamshetty, V., Nirmalakhandan, N., 2010. Fermentative biohydrogen production: Evaluation of net energy gain. Int. J. Hydrogen Energy 35, 12224–12233. https://doi.org/10.1016/j.ijhydene.2010.08.037

ROBERTA RE, NICOLETTA PELLEGRINI, ANNA PROTEGGENTE, ANANTH PANNALA, MIN YANG, A., RICE-EVANS, C., 1999. ANTIOXIDANT ACTIVITY APPLYING AN IMPROVED ABTS RADICAL CATION DECOLORIZATION ASSAY. Free Radic. Biol. Med. Vol. 26, 1231–1237.

Rodrigues, A.C., Boroski, M., Shimada, N.S., Garcia, J.C., Nozaki, J., Hioka, N., 2008. Treatment of paper pulp and paper mill wastewater by coagulation-flocculation followed by heterogeneous photocatalysis. J. Photochem. Photobiol. A Chem. 194, 1–10. https://doi.org/10.1016/j.jphotochem.2007.07.007

Roman, H.J., Burgess, J.E., Pletschke, B.I., 2006. Enzyme treatment to decrease solids and improve digestion of primary sewage sludge. African J. Biotechnol. 5, 963–967.

https://doi.org/10.5897/AJB06.154

Roy Ghatak, H., 2006. Electrolysis of black liquor for hydrogen production: Some initial findings. Int. J. Hydrogen Energy 31, 934–938. https://doi.org/10.1016/j.ijhydene.2005.07.013

Safatian, F., Doago, Z., Torabbeigi, M., Rahmani Shams, H., Ahadi, N., 2019. Lead ion removal from water by hydroxyapatite nanostructures synthesized from egg sells with microwave irradiation. Appl. Water Sci. 9, 1–6. https://doi.org/10.1007/s13201-019-0979-8

Salem, A.H., Mietzel, T., Brunstermann, R., Widmann, R., 2017. Effect of cell immobilization, hematite nanoparticles and formation of hydrogen-producing granules on biohydrogen production from sucrose wastewater. Int. J. Hydrogen Energy 42, 25225–25233. https://doi.org/10.1016/j.ijhydene.2017.08.060

Sari, A.A., Hanifah, U., Parmawati, Y., Permadi, R., 2018. Development of immobilized activated carbon-enzyme for decolorization of black liquor. Key Eng. Mater. 775 KEM, 402–407. https://doi.org/10.4028/www.scientific.net/KEM.775.402

Shaaban, A., Se, S.M., Mitan, N.M.M., Dimin, M.F., 2013. Characterization of biochar derived from rubber wood sawdust through slow pyrolysis on surface porosities and functional groups. Procedia Eng. 68, 365–371. https://doi.org/10.1016/j.proeng.2013.12.193

Soltan, M., Elsamadony, M., Mostafa, A., Awad, H., Tawfik, A., 2019. Harvesting zero waste from co-digested fruit and vegetable peels via integrated fermentation and pyrolysis processes. Environ. Sci. Pollut. Res. 26. https://doi.org/10.1007/s11356-019-04647-8

Tang, Y., Shigematsu, T., Morimura, S., Kida, K., 2005. Microbial community analysis of mesophilic anaerobic protein degradation process using bovine serum albumin (BSA)-fed continuous cultivation. J. Biosci. Bioeng. 99, 150–164. https://doi.org/10.1263/jbb.99.150

Torrades, F., Saiz, S., García-Hortal, J.A., García-Montaño, J., 2008. Degradation of wheat straw black liquor by Fenton and photo-Fenton processes. Environ. Eng. Sci. 25, 92–98. https://doi.org/10.1089/ees.2007.0021

Turon, P., del Valle, L.J., Alemán, C., Puiggalí, J., 2017. Biodegradable and biocompatible

systems based on hydroxyapatite nanoparticles. Appl. Sci. 7. https://doi.org/10.3390/app7010060

Vaez, E., Taherdanak, M., Zilouei, H., 2017. Dark Hydrogen Fermentation From Paper Mill Effluent (PME): The influence of Substrate Concentration and Hydrolysis. Environ. Energy Econ. Res. 1, 163–170. https://doi.org/10.22097/eeer.2017.47243

Van Der Waarde, J., Krooneman, J., Geurkink, B., Van Der Werf, A., Eikelboom, D., Beimfohr, C., Snaidr, J., Levantesi, C., Tandoi, V., 2002. Molecular monitoring of bulking sludge in industrial wastewater treatment plants. Water Sci. Technol. 46, 551–558. https://doi.org/10.2166/wst.2002.0533

Velioglu, Y.S., Mazza, G., Gao, L., Oomah, B.D., 1998. Antioxidant Activity and Total Phenolics in Selected Fruits , Vegetables , and Grain Products 4113–4117. https://doi.org/10.1021/jf9801973

Wen, T., Wu, X., Liu, M., Xing, Z., Wang, X., Xu, A.W., 2014. Efficient capture of strontium from aqueous solutions using graphene oxide-hydroxyapatite nanocomposites. Dalt. Trans. 43, 7464–7472. https://doi.org/10.1039/c3dt53591f

Yang, G., Zhang, P., Zhang, G., Wang, Y., Yang, A., 2015. Degradation properties of protein and carbohydrate during sludge anaerobic digestion. Bioresour. Technol. 192, 126–130. https://doi.org/10.1016/j.biortech.2015.05.076

Yu, H., Zhu, Z., Hu, W., Zhang, H., 2002. Hydrogen production from rice winery wastewater in an up ow anaerobic reactor by using mixed anaerobic cultures 27, 1359–1365.

Yuan, Z., Yang, H., Zhi, X., Shen, J., 2010. Increased performance of continuous stirred tank reactor with calcium supplementation. Int. J. Hydrogen Energy 35, 2622–2626. https://doi.org/10.1016/j.ijhydene.2009.04.018

Yuan, Z., Yang, H., Zhi, X., Shen, J., 2008. Enhancement effect of l-cysteine on dark fermentative hydrogen production. Int. J. Hydrogen Energy 33, 6535–6540. https://doi.org/10.1016/j.ijhydene.2008.07.065

Zeng, Z., Li, Y., Yang, R., Liu, C., Hu, X., Luo, S., Gong, E., Ye, J., 2017. The relationship

between reducing sugars and phenolic retention of brown rice after enzymatic extrusion. J. Cereal Sci. 74, 244–249. https://doi.org/10.1016/j.jcs.2017.02.016

Zhang, Lei, Zhang, Lixia, Li, D., 2015. Enhanced dark fermentative hydrogen production by zero-valent iron activated carbon micro-electrolysis. Int. J. Hydrogen Energy 40, 12201–12208. https://doi.org/10.1016/j.ijhydene.2015.07.106

Zhao, W., Zhao, J., Chen, G., Feng, R., Yang, J., Zhao, Y., Wei, Q., Du, B., Zhang, Y., 2011. Anaerobic biohydrogen production by the mixed culture with mesoporous Fe3O4 nanoparticles activation. Adv. Mater. Res. 306–307, 1528–1531. https://doi.org/10.4028/www.scientific.net/AMR.306-307.1528

Figure
Click here to download Figure: 2_List of figures_M.docx

List of figures

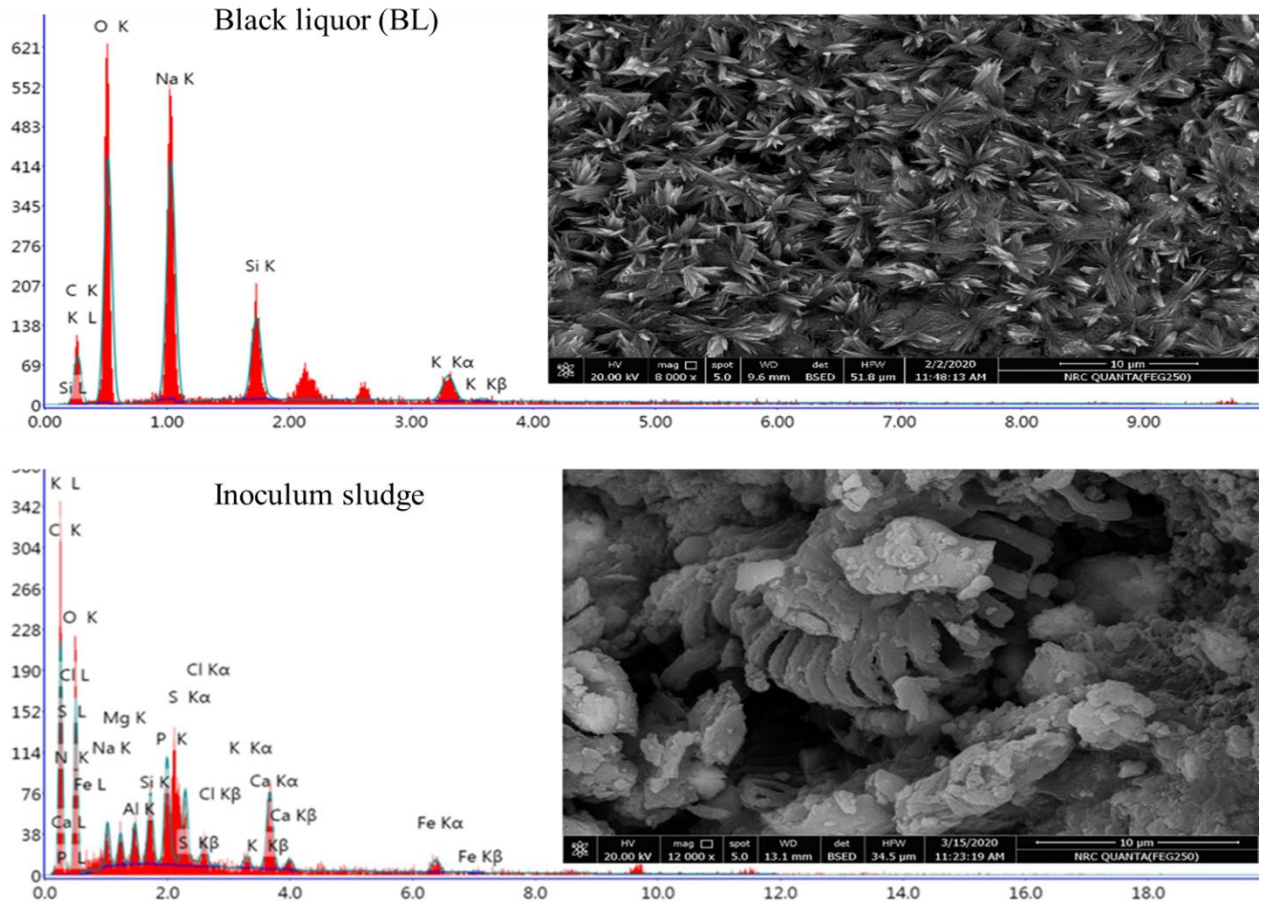

Fig. 1a scanning electron microscope (SEM) image and energy dispersive X-Ray (EDX) analysis of the black liquor (BL) and inoculum sludge

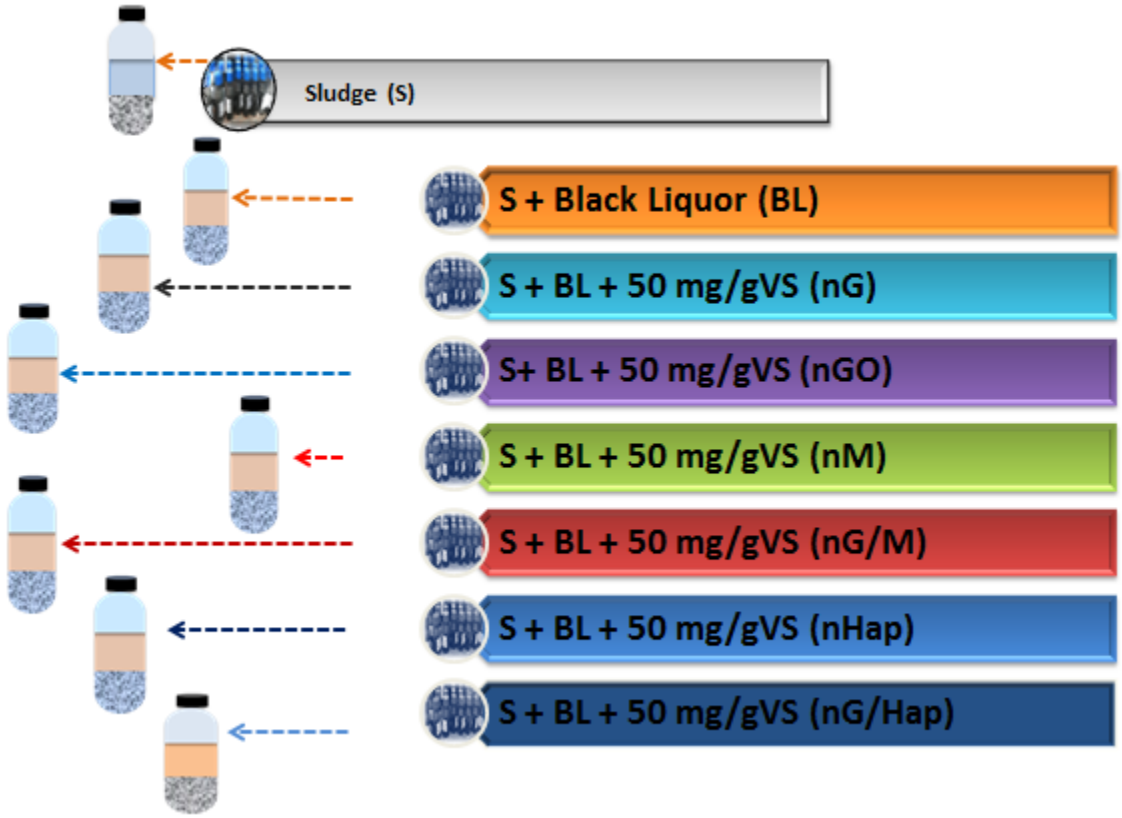

Fig. 1b experimental set-up of anaerobic batch assays

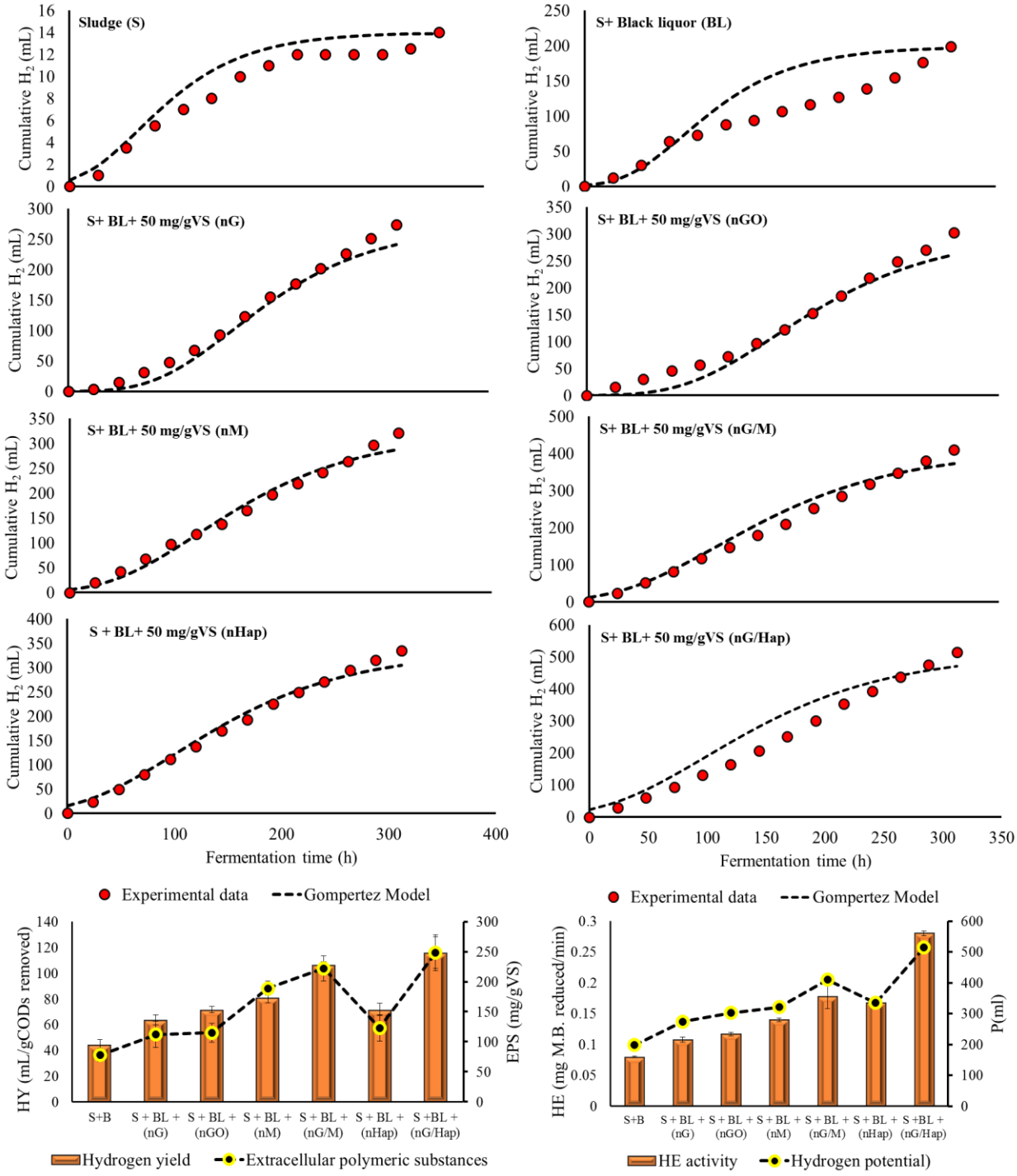

Fig. 2a the experimental and modeled data for bio-H_2 production based on modified Gompertz equation, hydrogen yield (HY) versus extracellular polymeric substances (EPS), hydrogenase enzyme (HE) activity versus hydrogen potential (P)

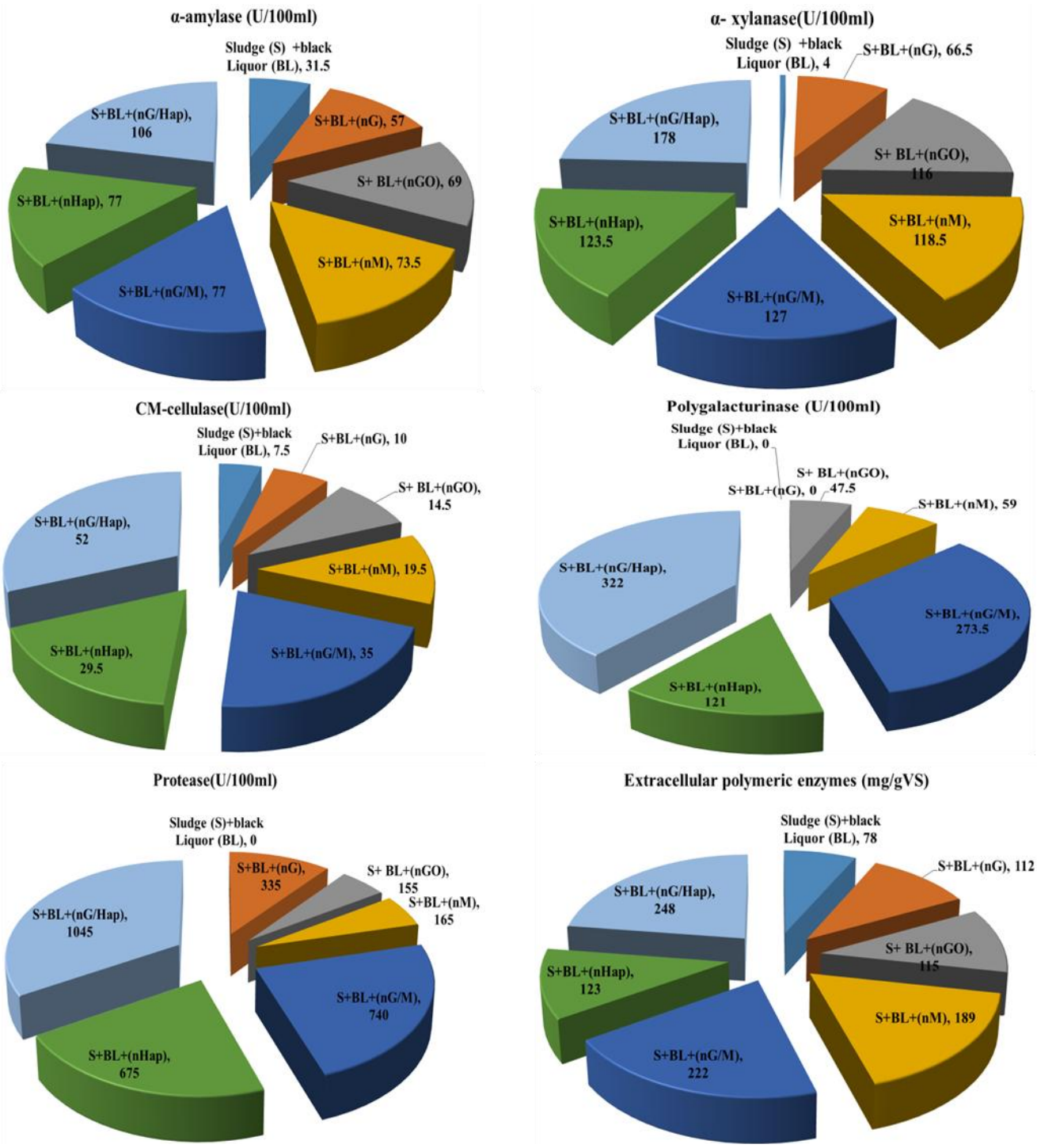

Fig. 2b enzymatic activities for anaerobes with free and combined nanoparticles for degradation of black liquor (BL)

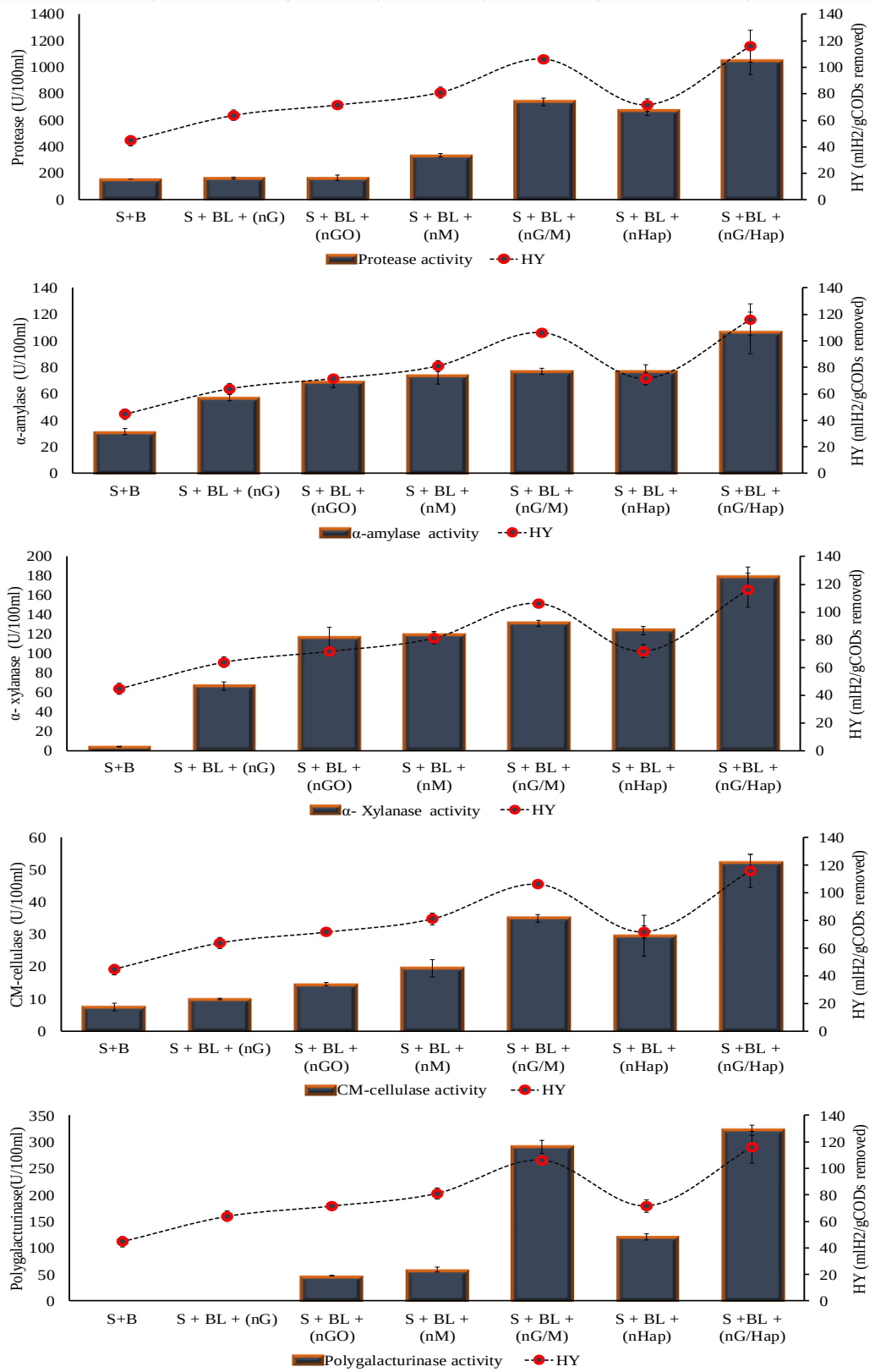

Figs. 3a enzymatic activities and hydrogen yield (HY) for solely and dual nano-particles

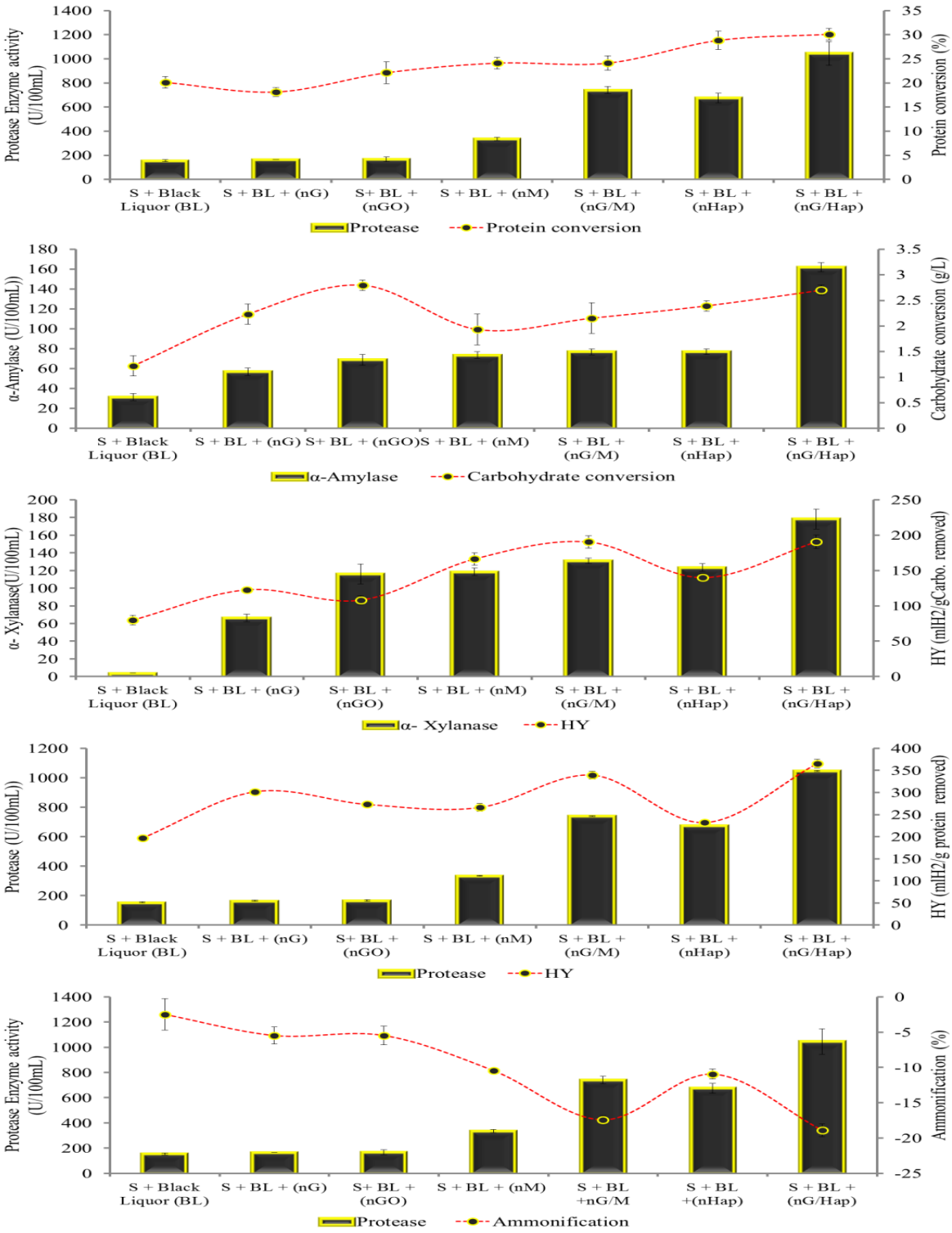

Figs. 3b conversion of proteins, carbohydrates, CODs, ammonification process and hydrogen yield (HY) for anaerobes supplemented with solely and dual nano-particles

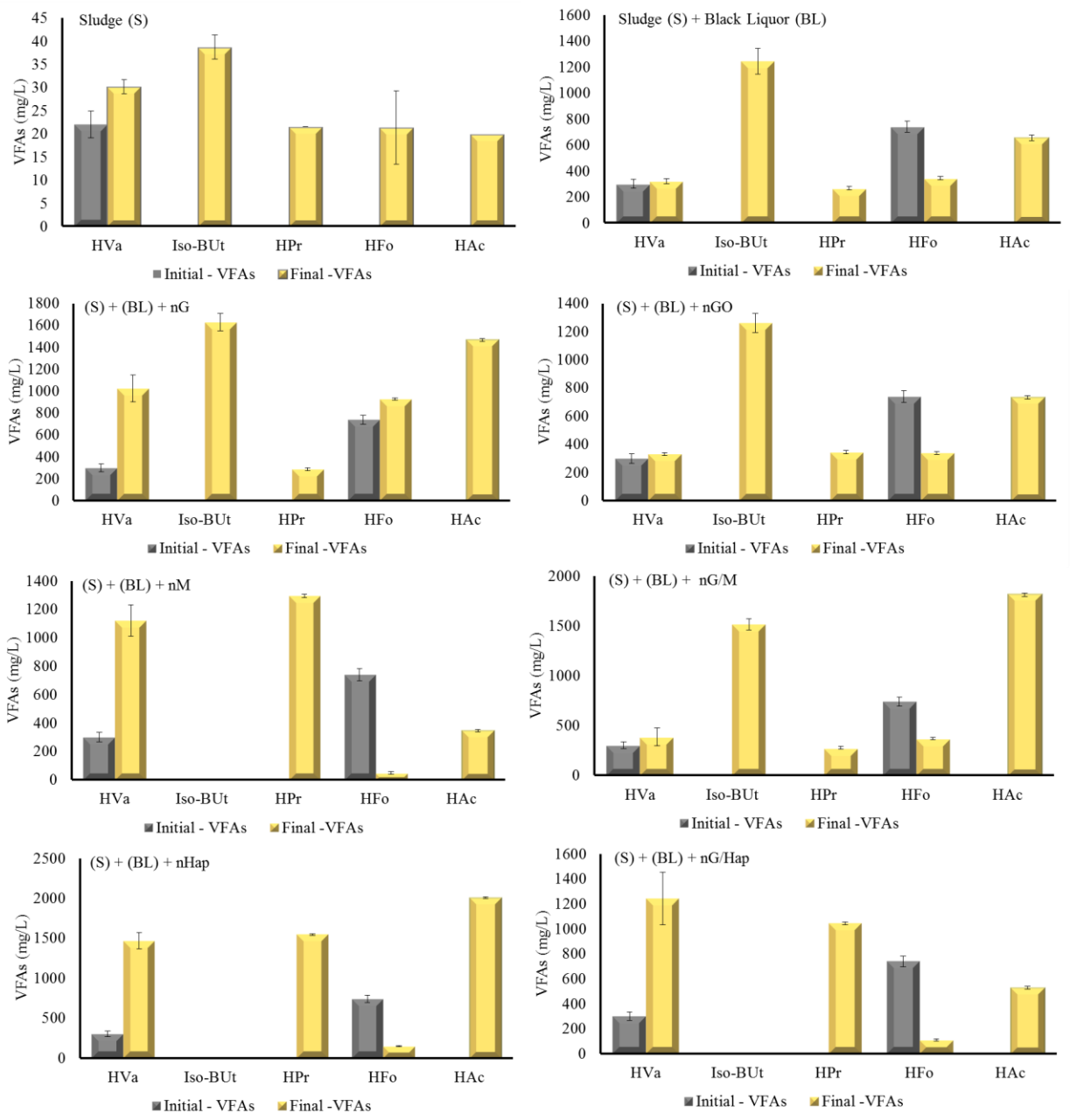

Fig. 3c metabolite by-products of the anaerobes producing hydrogen supplemented with solely and dual nano- particles from black liquor

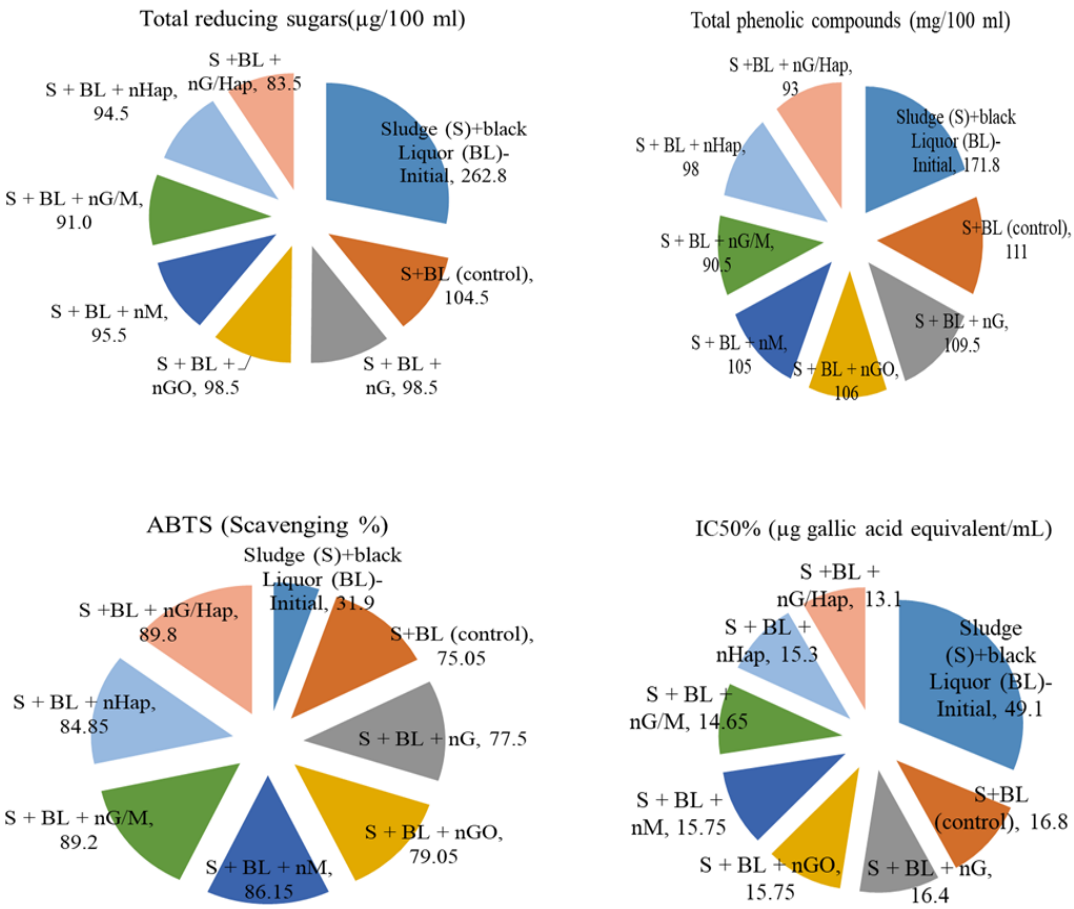

Fig. 3d total reducing sugars, total phenolic compounds, antioxidant activities –ABTS and the half maximal inhibitory concentration **(**IC_{50}) of anaerobes with free and combined nanoparticles for degradation of black liquor

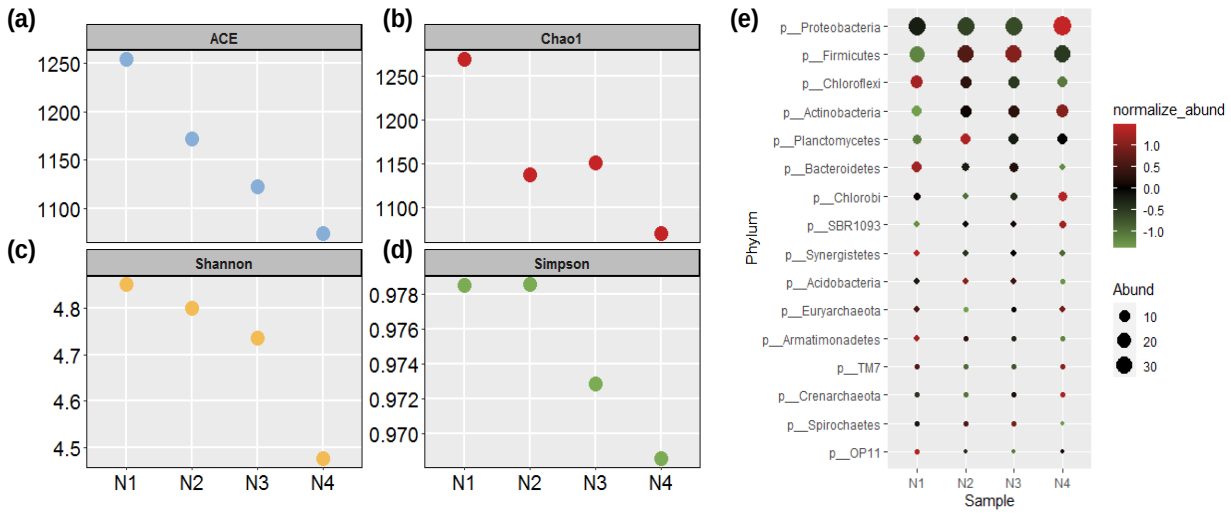

Fig. 4 Alpha-diversity and community structure of sludge supplemented with nG/Hap, nG/M, nM and nHap (N1, N2, N3 and N4). The ACE (a) and Chao1(b) indices are related to the absolute number of species in a given culture, while Simpson (c) and Shannon (d) indices are belong to the distribution of species abundance of microbial communities. The major phyla (>0.1%) of the anaerobes (e) in the anaerobes immobilized on nanopartiles (N1,N2, N3 and N4). The size of the circle is proportional to the relative abundances of phyla in the digester. The color scale indicates the normalized relative abundances of phyla.

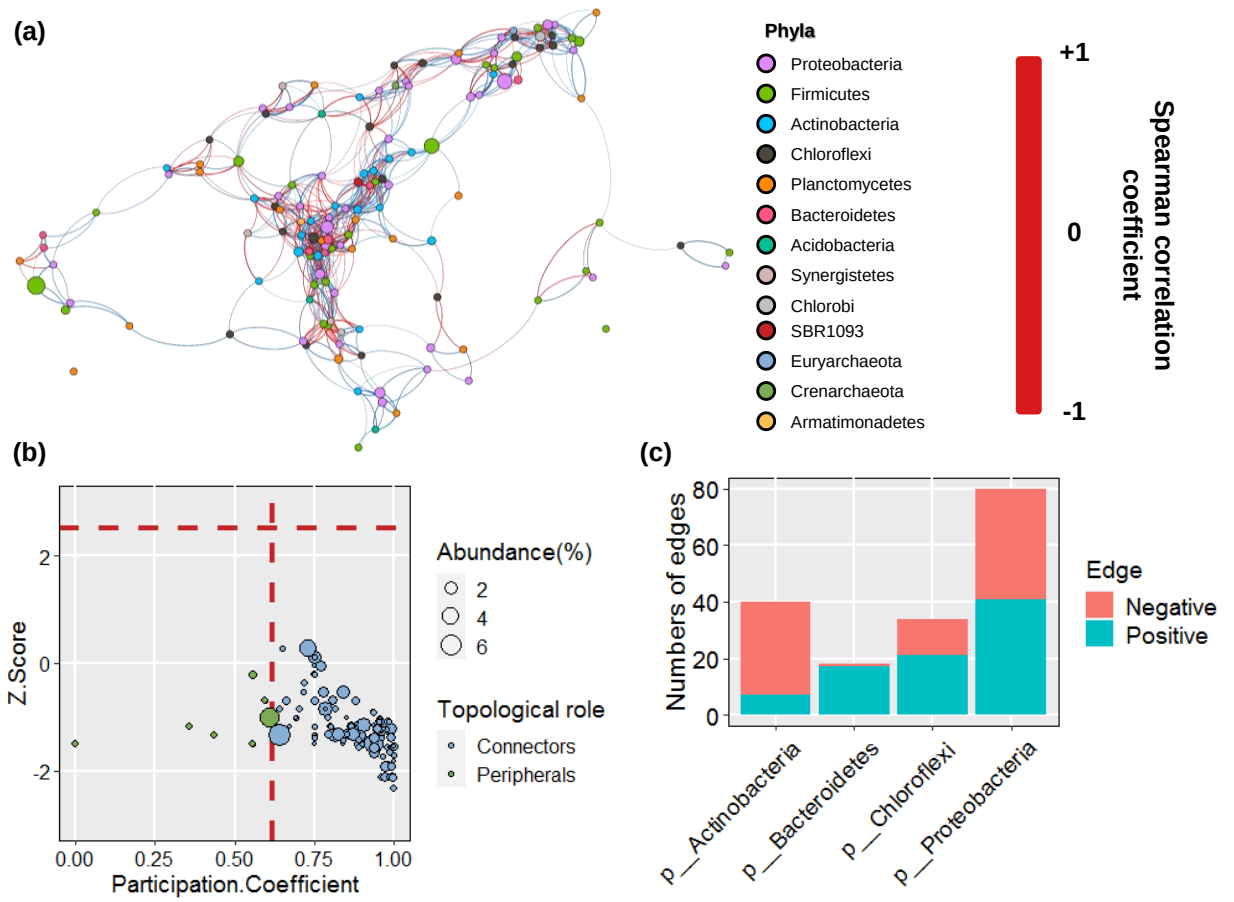

Fig. 5 community ecology of the anaerobes (a) Phyla network uncovered the co-occurrence and co-exclusion between OTUs. Only the major OTUs (average abundance > 0.1%) and statistically significant correlations (*P*-value p0.05) are shown, resulting in the network consisted of 139 nodes and 774 edges. The size of the node is proportional to the RA of phylum in the digester and the node color represents the affiliated phylum of the node. Red and blue edges represent the co-exclusion and co-occurrence respectively. The wider edge gives an indication for the stronger correlations. (b) ZP-plot showing distribution of OTUs based on their module-based topological roles. The size of the circle is proportional to the average RA of phylum in the samples. (c) Numbers of positive and negative edges between the OTUs affiliated with *Firmicutes* and other major phyla.

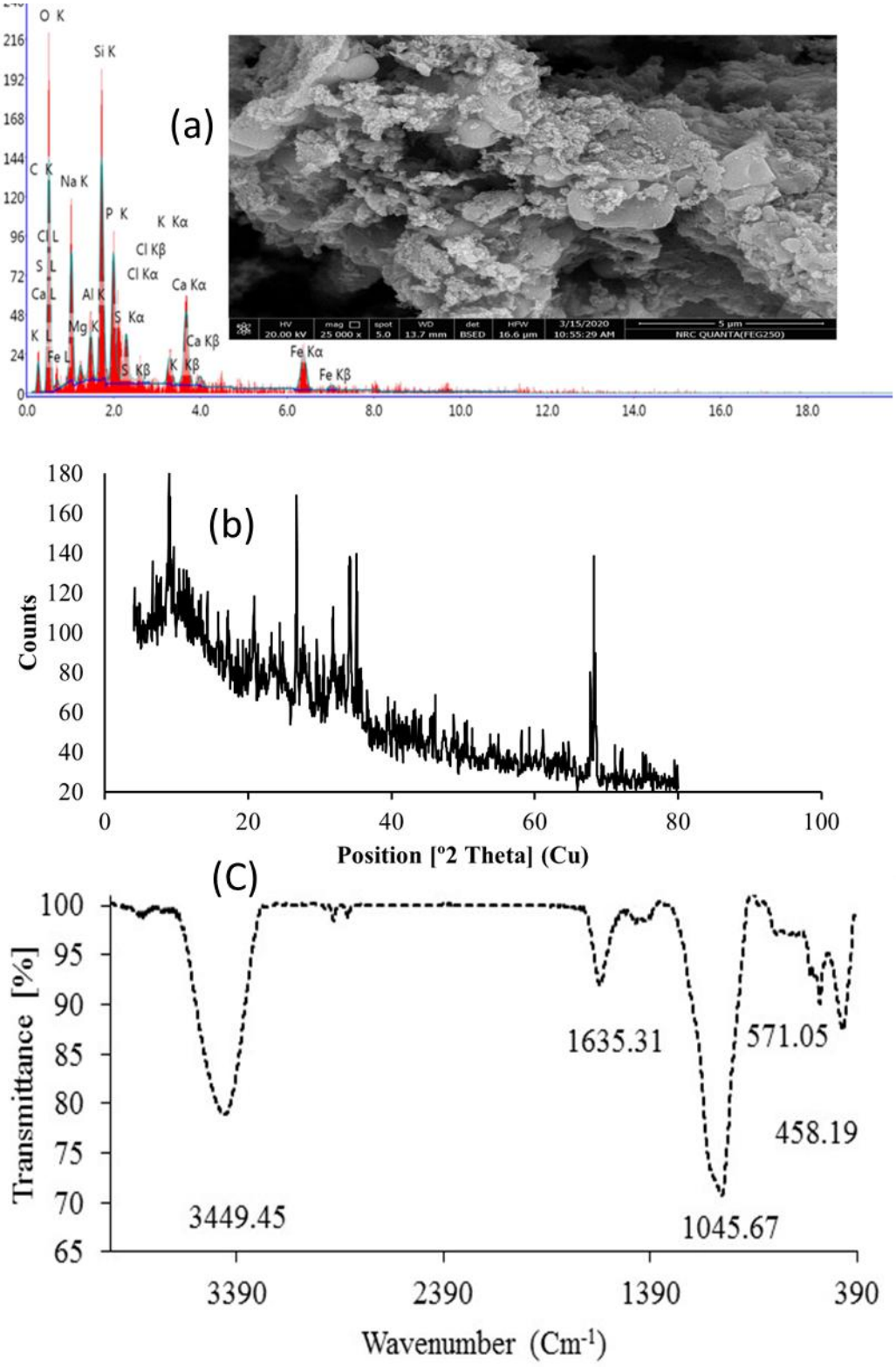

Fig. 6 scanning electron microscopy (SEM), Energy dispersive X-ray (EDX) (a), infrared absorption spectroscopy (FTIR) (b) and diffractometry of X- rays (XRD) (c) of the bio-char

List of tables

Table 1a black liquor (Bl) and inoculum sludge (S) characteristics (Values ±Stdv)

Parameters	Black Liquor (BL)	Inoculum sludge (S)
pH-value	12.75±2.1	7.8±0.2
CODt -g/L	22.3±0.6	70.75±0.67
CODs - g/L	21.88±0.45	3.68±0.03
CODp - g/L	0.42±0.05	67.07±0.06
CODs/CODt ratio	0.98	0.05
CODp/CODt ratio	0.02	0.95
TOC - g/L	8.26±0.23	26.20±0.13
Total solids (TS) - g/L	43.8±0.23	132.04±0.34
Volatile solids (VS) - g/L	21.85±0.56	72.75±035
VS/TS ratio	0.50	0.55
Total phosphorous (TP) - g/L	5.79±0.30	2.11±0.08
C/P ratio	3.85	33.53
TKJ-N - g/L	1.82±0.09	5.32±0.15
C/N ratio	12.25	13.30
Protein - g/L	11.36±0.46	33.2±1.9
Carbohydrates- g/L	43.5±12.7	52.2±0.9
Total reducing sugars (TRS) - mg/L	262.8±11.9	0.1±0.001
Total phenolic compounds (TPC) - mg/L	1718±12.4	-
TRS/TPC ratio	0.15	-
Valerate (HVa)- mg/L	2234±56.9	22±2.9
Iso-butyrate (HBu)- mg/L	ND*	ND*
Propionate (HPr) - mg/L	ND*	ND*
Formate (HFo) - mg/L	2033±112	ND*
Acetate (HAc) - mg/L	ND*	ND*
The half maximal inhibitory concentration (IC_{50}) (µg Gallic acid equivalent/ mL)	48.4±0.3	1.1±0.08
Antioxidant activity -ABTS (scavenging %)	31.9±2.9	-
α-amylase- U/100 mL	ND*	9.0±0.4
α- xylanase (used breach xylan)- U/100 mL	ND*	400±7.8
α- xylanase (used birch xylan)- U/100 mL	ND*	15±1.2
CM-cellulase (used filter paper)- U/100 mL	ND*	ND*
CM-cellulase (CM-cellulose)- U/100 mL	ND*	4.1±0.7
Polygalacturonase- U/100 mL	ND*	ND*
Peroxidase- U/100 mL	ND*	ND*
Protease - U/100 mL	ND*	165±6.9
Crystallinity index (%)	29.5	-

ND*: not detected

Table 1b energy dispersive X-Ray (EDX) analysis of the black liquor and inoculum sludge

Elements	Black Liquor (BL)				Inoculum sludge			
	Weight %	Atomic %	Net Int.	Error %	Weight %	Atomic %	Net Int.	Error %
Carbon (C)	21.06	29.44	19.57	13.6	44.39	55.91	51.56	10.93
Oxygen (O_2)	44.82	47.03	110.99	9.93	30.96	29.28	42.1	12.9
Sodium (Na)	26.59	19.42	118.88	8.84	2.59	1.71	11.76	15.24
Silica (Si)	5.2	3.11	45.78	8.99	1.82	0.98	21.37	10.75
Potassium (K)	2.32	1.0	17.25	13.35	0.58	0.22	4.9	29.4
Nitrogen (N)	--	--	--	--	5.12	5.53	2	37.2
Magnesium (Mg)	--	--	--	--	1.04	0.64	8.42	20.18
Aluminum (AL)	--	--	--	--	1.12	0.63	11.24	15.55
Phosphorous (P)	--	--	--	--	3.19	1.56	32.64	8.52
Sulfur (S)	--	--	--	--	2.36	1.11	25.15	10.96
Chlorine (Cl)	--	--	--	--	0.95	0.41	9.29	18.36
Calcium (Ca)	--	--	--	--	4.1	1.5	29.1	9.1
Iron (Fe)	--	--	--	--	1.8	0.5	5.9	24.3

Table 2 chemical and textural characteristics for the bio-char

Element	Weight %	Atomic %	Net Int.	Error %
Carbon (C)	13.73	22.5	4.23	22.08
Oxygen (O)	37.44	46.07	36.64	12.37
Sodium (Na)	11.98	10.26	23.41	12.91
Magnesium (Mg)	0.95	0.77	2.89	63.35
Aluminum (Al)	2.32	1.7	9.11	19.35
Silica (Si)	9.18	6.43	43.07	8.92
Phosphorous (P)	6.48	4.12	25.36	11.12
Sulfur (S)	2.43	1.49	10.14	18.33
Chlorine (Cl)	0.64	0.35	2.55	65.23
Potassium (K)	1.72	0.87	6.39	22.88

Anaerobes supplemented with solely/dual nano-particles for bio-(H_2&char) production from black liquor

Mohamed El-Qelish[1], Aida Galal[1], Zhong Yu[2], Mohamed A. Hassan[3], H. A. Salah[4], Mohamed S. Hasanin[5], Fangang Meng[2], Ahmed Tawfik[1♥]

[1] National Research Centre, Water Pollution Research Department, 12622, Dokki, Cairo, Egypt

[2]School of Environmental Science and Engineering, Sun Yat-sen University, Guangzhou 510006, PR China

[3]Agricultural Research Centre, Nanotechnology and Advanced Material Central Lab., Giza, Egypt

[4]National Research Centre, Molecular Biology Department, 12622, Dokki, Cairo, Egypt

[5]National Research Centre, Cellulose and Paper Department, 12622, Dokki, Cairo, Egypt

♥ Corresponding author: qelish88@yahoo.com (Mohamed El-Qelish)

1. *Preparation of solely and dual nanoparticles*

Analytical grade chemicals were purchased from Sigma Aldrich for preparation of graphene oxide (nGO), graphene (nG), Magnetite (nM), graphene/magnetite (nG/M), hydroxyapatite (nHap) and graphene/hydroxyapatite (nG/Hap) at a nano-scale. A modified Hummers method was used to synthesize nGO in nano-scale from graphite powder as carbon precursor as previously described earlier by Chen (Chen et al., 2013).

Graphene nano-sheets were prepared using the solvothermal method using ethylene glycol and graphene oxide (GO). 1.5 g of the previously prepared nGO was suspended in ethylene glycol (240 ml) and strongly sonicated for 15 min. in ultrasonic waves equipped with probe. The suspension was carefully transferred in a stainless steel Teflon lined autoclave and incubated for a period of 24 h., at a temperature of 180 ºC. The black solution was produced, immediately washed and filtrated several times by deionized H_2O and Et-OH. The mixture was allowed to be dried overnight at a temperature of 70 °C.

Magnetite nanoparticles (nM) were prepared under continuous nitrogen gas flow. 0.82725 g of ferric chloride ($FeCl_3$, M.Wt 162.2) and 1.0 g of ammonium ferrous sulfate $(NH_4)_2Fe(SO_4)_2.6H_2O$, was added to a 50 ml solution of NaOH (3.0 M) and continuously stirred to complete solubilization of the iron salts in the reaction medium. A brown color is formed at pH value of 2-3 which was further increased up to 10.0 using NaOH solution (3.0 M) resulting a black color precipitate. The latter was carefully filtrated, washed several times with deionized H_2O and dried at a temperature of 35 °C for 24h.

Graphene/magnetite (nG/M) was prepared and synthesized using Solvothermal method where 5.0 g of sodium acetate was added to an ultrasonicated graphene oxide solution (0.5 g) and mixed in 80 ml ethylene glycol. 0.42 g $FeCl_3$ was added to the previous solution under continuous flow of nitrogen gas. This mixture was carefully transferred into an autoclave Teflon-lined stainless steel and heated at a temperature of 200 °C for a period of 10 h. The obtained black powder was washed several times with Et-OH and deionized H_2O, then dried in a vacuum oven at a temperature of 60 °C.

Hydroxyapatite nanoparticles (nHap) was prepared based on a stoichiometric molar ratio of 1.67 (Ca/P), by addition of 0.8 mol. (Ca $(NO_3)_2.4H_2O$ and 0.479 mol H_3PO_4 in a sol-gel method. Ammonia solution was used to adjust the pH value at a level of 10.0±0.05. Ca $(NO_3)_2.4H_2O$ solution was vigorously stirred at a temperature of 25 °C and phosphoric acid was drop-wisely

added at a flow rate of 3 ml/min. The suspension was left under vigorous stirring for a time of 16 h., and after 24 h., of aging, the precipitate was rinsed with deionized H_2O and dried at a temperature of 100 °C under vacuum.

Graphene/ hydroxyapatite (G/nHap) was prepared by hydrothermal treatment of the mixture of 600 mg of nGO, 8 mM of $CaCl_2$, 4.8 mM $(NH_4)_2(HPO_4)$ and the pH value of 10.0 was adjusted using ammonium hydroxide. Afterwards, the mixture was heated in a stainless steel Teflon lined autoclave at a temperature of 180 °C for a period of 24 h. The composite was regularly separated using centrifugation, washed by distilled H_2O & Et-OH ethanol and dried overnight at a temperature of 70 °C.

2. Characterization of solely and dual nanoparticles

Immobilization of anaerobes degrading organics on the nano-particles (nPs) is a promising approach where the H_2 yield (HY) is improved due to an increase of hydrogenase enzyme as described earlier by Elreedy et al., (2017). Moreover, metal nPs represented a source of nutrients for micro-organisms at appropriate doses where Han et al., (2011) found a gradual release of iron from hematite nPs in the reaction medium. Solely and dual nano-particles (nPs) i.e. graphene oxide (nGO), graphene (nG), magnetite (nM), graphene/magnetite (nG/M), hydroxyapatite (nHap) and graphene/hydroxyapatite (nG/Hap) was attempted for enhancement of hydrogen fermentative of black liquor (BL). The characteristics of solely and dual nano-particles (nPs) are presented in **Fig. s1.** The prepared graphene nanoparticles (nG) revealed disordered structure which is reflected by the broad X-ray diffraction peaks centered at approximately 2θ of 19°which corresponds to the (002) reflection of graphene. The broad (002) peak revealed that the graphene is not crystalline as graphite as shown in **Fig. s1.** The XRD pattern of nHap showed several signals at 2θ of 25.88°, 31.88°, 32.28°, 34.08°, 39.78° and 49.58°, corresponding to the diffraction planes (0 0 2), (2 1 1), (1 1 2), (2 0 2), (1 3 0) and (2 1 3), respectively (JCPDS no.01-073- 8417). Those signals confirmed the deposition of nHAP in a hexagonal structure.

Fourier transform infra-red (FTIR) spectra of nGO is illustrated in **Fig. s1.** GO spectrum showed peaks at 1046, 1445, 1629, 2924 and 3430 cm^{-1} as earlier reported by Kyzas et al.,(Kyzas et al., 2013). The intense, broad band at 3430 cm^{-1} is attributed to O-H stretching of the hydroxyl and carboxyl groups of GO, in addition to the residual water between the GO sheets. Peaks at 1046

and 1445 cm^{-1} is attributed to the stretching of epoxy group, whereas peak at 1629 cm^{-1} were due to the C=O stretching in the carbonyl and carboxylic groups (Chen et al., 2013). These hydrophilic oxygen-containing functional groups provided GO sheets highly dispensable in water, resulting formation of hydrogen bonds between the graphite and water molecules. Magnetite (nG) provided an intense peak at 562 cm^{-1} which is attributed to the stretching vibrational mode due to metal-oxygen Fe-O bonds in the crystalline lattice of Fe_3O_4 (Nalbandian et al., 2015). Bands at 1636 and 3433 cm^{-1} are related to the hydroxyl group and confirms the presence of OH-bending and OH-stretching group, respectively. FTIR spectrum of nHap illustrated a characteristic absorption peaks (**Fig. s1**). The broad bands were detected at 3430 and 1633 cm^{-1} which could be attributed to the adsorbed water. Bands at peaks of 589 and 1048 cm^{-1} were appeared for PO_4^{3-} group(Cengiz et al., 2008).

The SEM imaging of nG sheets are presented in **Fig. s2.** The image showed a layered structure with a fluffy appearance and highly agglomeration of the sheets. nGO morphology under SEM micrograph showed a crumpled and rippled structure due to the deformation upon exfoliation as shown in **Fig. s2**. The multilayered structure is clearly observed. Magnetite (nM) was appeared to be very fine powder configuration with mono-dispersed nature **(Fig. s2).** The particles seem to be scattered with no signs of aggregation (Al-Jabri et al., 2018). Morphology of the nHap showed a powder configuration with rod shaped nanoparticles with no evidence of agglomeration (**Fig. s2).** Energy dispersive X-ray (EDX) analysis of the nG, nGO, nM, nHap, nG/M and nG/Hap are presented in **Table s1.** The starting molar ratio of calcium to phosphorus was (1.67) in nHap which are confirmed by the results of EDX analysis. Likely, high quantity of carbon (70.4) and low portion of oxygen (29.66) are observed for nG. The oxygen atoms were still detected in the nG sheets structure which strongly indicates the occurring of reduction of graphene oxide into nG sheets. However, the reduction process was not fully accomplished due to the presence of other oxygen groups in the graphene structure. The atom ratio of C: O in nGO was in consistence with the original precursors which estimated to be 4:5 (0.8). The appearance of the sulfur (2.05%) in the spectrum of nGO was due to the use H_2SO_4 as oxidizing agent. The EDX analysis of nM revealed pure Fe_3O_4 nanoparticles where the composition analysis was 69.44% for Iron and 30.56 % for oxygen. This result demonstrates the high purity of the magnetite nanoparticles (nM). The data for composition of nG/Hap was satisfactory where carbon, oxygen, phosphorous and calcium were 28.48, 35.73, 11.34 and 24.45% respectively.

Fig. s2 shows the transmission electron microscopy (TEM) imaging of nG, where a few layers of relatively transparent sheets was entangled and rippled with each other. nG/Hap showed the crystallization thin shape (ca. 20 nm in diameter), short in length (30–50 nm) and nano-rods with minor aggregations. The electron diffraction pattern (inset of **Fig. s2**) showed polycrystalline diffraction rings of nG/Hap composite.

3. Microbial analysis community

3.1. DNA extraction

The batch samples supplemented with nG/Hap, nG/M, nM and nHap (denoted as N1, N2, N3 and N4, respectively) were aliquoted after fermentation and stored at -20 ºC for DNA analysis. Cells were pelleted by centrifugation (6000g, 10 min) before DNA extraction. The Macherey Nagel NucleoSpin Soil kit was used for DNA extraction from 300 mg of pellet according to the manufacturer's instructions. The extracted DNA was carefully eluted in 100 µL of sterile water and stored at temperature of -20°C for further analysis. Spectrophotometry (ND-1000, Nanodrop Tech.) was thoroughly used to check the concentration and purity of DNA and subsequently, DNA quality was determined on 0.7% agarose gel in Tris Borate EDTA (TBE) 1X Buffer.

3.2. Quantitative PCR (qPCR)

The archaeal and bacterial communities of each sample were quantified using qPCR techniques targeting the 16S rRNA gene. All qPCR amplifications were determined according to the supplier's instructions using CFX thermal cycler (BioRad). The mixtures of 25 µL contained 12.5 µL of iQ Sybr Green supermix 2X (BioRad), 1.5 µL (10 µM) of each primer set 1055F (5'-ATGGCTGTCGTCAGCT-3') and 1392R (5'-ACGGGCGGTGTGTAC-3') for bacteria or 0.5 µL (10 µM) of ARC787F (5'-ATTAGATACCCSBGTAGTCC-3') and ARC1059R (5'-GCCATGCACCWCCTCT-3') for archaea, 2 µL of template DNA, and the remaining portion as sterile water. The amplification reaction process for bacterial communities was: initial denaturation at temperature of 94 °C for 10 min followed by 45 cycles of 95 °C for 30 s, 60 °C for 50 s, and 72 °C for 30s. The amplification reaction for Archaea was: initial denaturation at a temperature of 95 °C for 15 min, followed by 45 cycles of 95 °C for 15 s, 50 °C for 20 s, and 72°C for 1 min. Finally, a melting curve analysis was assessed to check the specificity of amplification and primer dimers formation. Standard curve was drawn up by 10-fold dilution of

an initial solution of bacterial community or archaeal PCR product with a known concentration. All samples and standards was carried out in triplicates and the gene copy numbers were estimated by comparison with DNA standards of known concentrations.

3.3. Community analysis using Single Strand Conformation Polymorphism (SSCP)

Bacterial community analysis was carried out by PCR-SSCP amplification as earlier described by Delbès et al. (Delbès et al., 2001). Bacterial primers W49 (5'-ACGGTCCAGACTCCTACGGG-3') and 5'FAM W34 (5'-FAM-TTACCGC GGCTGCTGGCAC-3') were efficiently used to target 200 bp of the 16S rRNA gene V3 region. Each PCR mixture contains 2.0 µL of 10X *Pfu* turbo DNA polymerase buffer (Agilent Technologies), 200 µM of each *dNTP*, 0.25 µM of each primer, 0.2 µL of *Pfu* turbo DNA polymerase (Agilent Technologies). The PCR reaction was carried out as follows: initial denaturation at temperature of 94 °C for 2 min, followed by 25 cycles at 94 °C for 30 s, 61°C for 30 s, 72 °C for 30s, with final step at 72°C for 10 min. Amplifications were assessed with a T100 thermal cycler (BioRad). One µL of diluted PCR product was mixed with 18.8 µL of formamide and 0.2 µL of internal standard 400HD Genescan ROX (Applied Biosystems). Samples were denatured at a temperature of 95 °C for 5 min and immediately cooled in the ice. Capillary-Electrophoresis-SSCP (CE-SSCP) was performed on ABI 310 Genetic Analyzer (Delbès et al., 2001).

3.4. OTU assignments and statistical analysis

The extracted DNA was further used for the amplification of the bacterial and archaeal hypervariable region V4–V5 of the 16S rRNA gene with primers 515F (5'-GTGYCAGCMGCCGCGGTA-3') and 928R (5'-CCCCGYCAATTCMTTTRAGT-3') as previously described by Poirier et al. (Poirier et al., 2016). The Quantitative Insights into Microbial Ecology (QIIME) software was used to analyze of the sequences (Wu et al., 2010). In particular, quality filtered sequence data was exported as FastQ file (15,000 to 90,000 reads for each sample). The quality of reads were carefully checked by three amplicon read processing pipelines i.e. MOTHUR v.1.25.0 (Schloss et al., 2009), QIIME 1.8.0 (Wu et al., 2010), and USEARCH v5.2.136 (Edgar, 2013). Low quality score (<20) and/or sequences shorter than 180 bp were removed. Chimeric sequences were totally removed and sequences were clustered into

Operational Taxonomic Units (OTUs) with 97% sequence similarity using quality filter (USEARCH) (http://www.drive5.com/usearch/) reference set(Edgar, 2010). A representative sequence for each OTU was selected based on the longest sequence in each OTU and assigned to the corresponding taxa using the Ribosomal Database Project (RDP) classifier. Furthermore, the Chao1, ACE, Simpson, and Shannon indices were calculated based on the rarefied OTU table using the package 'vegan' in R (Oksanen, J., Blanchet, F., Kindt, R., Legendre, P., O'hara, R., Simpson, G., Solymos, P., Stevens, M. and Wagner, 2011). The relative abundances of different phyla were calculated and display it in the bubble plot generated by package 'ggplot2'. We investigated the pair-wise Spearman's correlation coefficients among the major OTUs (average abundance > 0.1%), and created the network by software Gephi (Bastian, M., Heymann, S. and Jacomy, 2009). The number of edges connected to different phyla was summarized in R. The topological role of a node was characterized by its standardized within-module degree z and its among-module connectivity, p, using the plugin GIANT in Cytopscape (Cumbo et al., 2014; Paul Shannon et al., 1971). The nodes were sorted into peripherals, connectors, module hubs, and network hubs as previously described (Olesen et al., 2007).

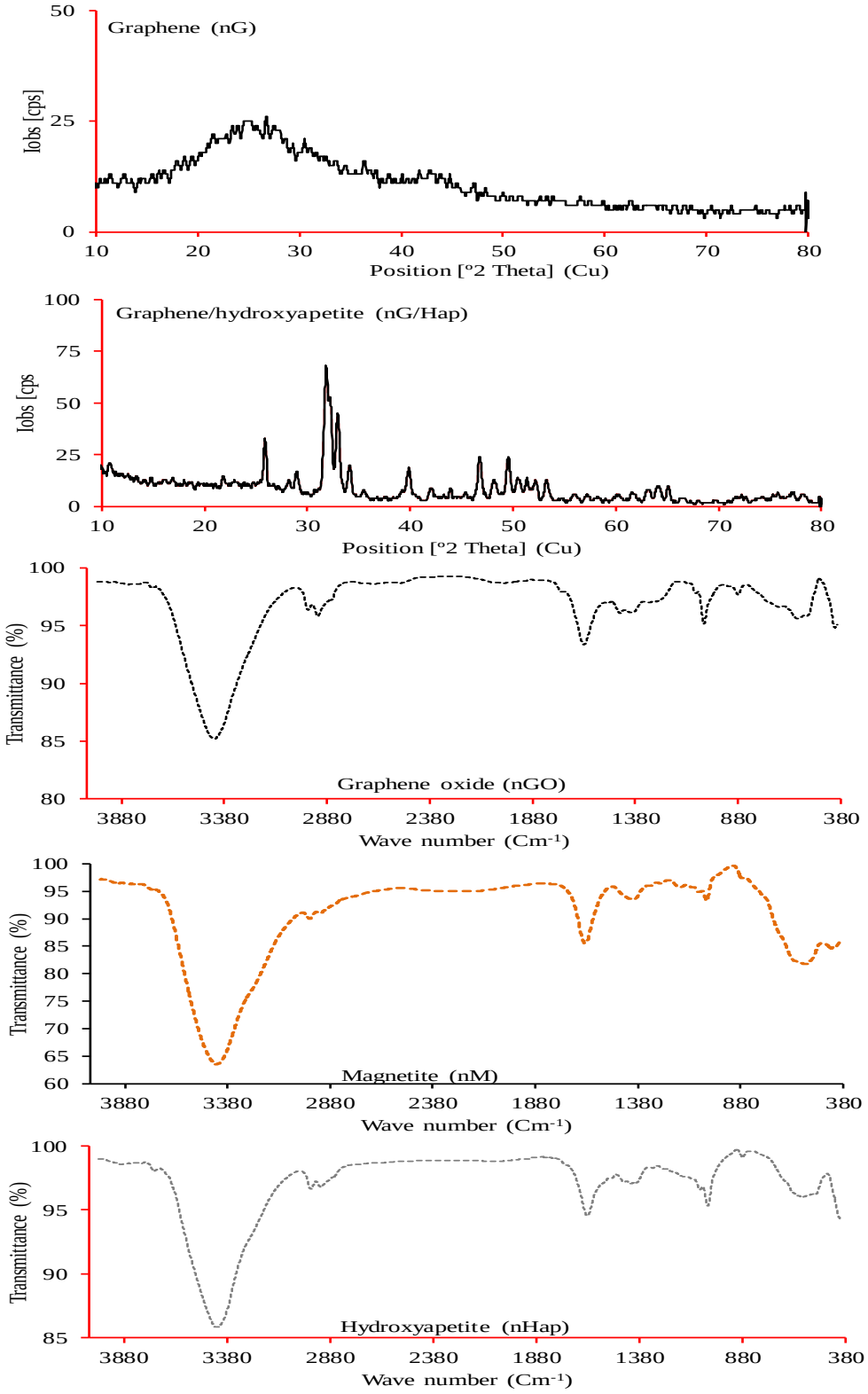

Fig. S1 X-ray diffraction (XRD) for Graphene (nG) and Graphene/hydroxyapatite (nG/Hap) & Fourier transform infra-red (FTIR) spectra for graphene oxide (nGO), magnetite (nM) and hydroxyapatite (nHap)

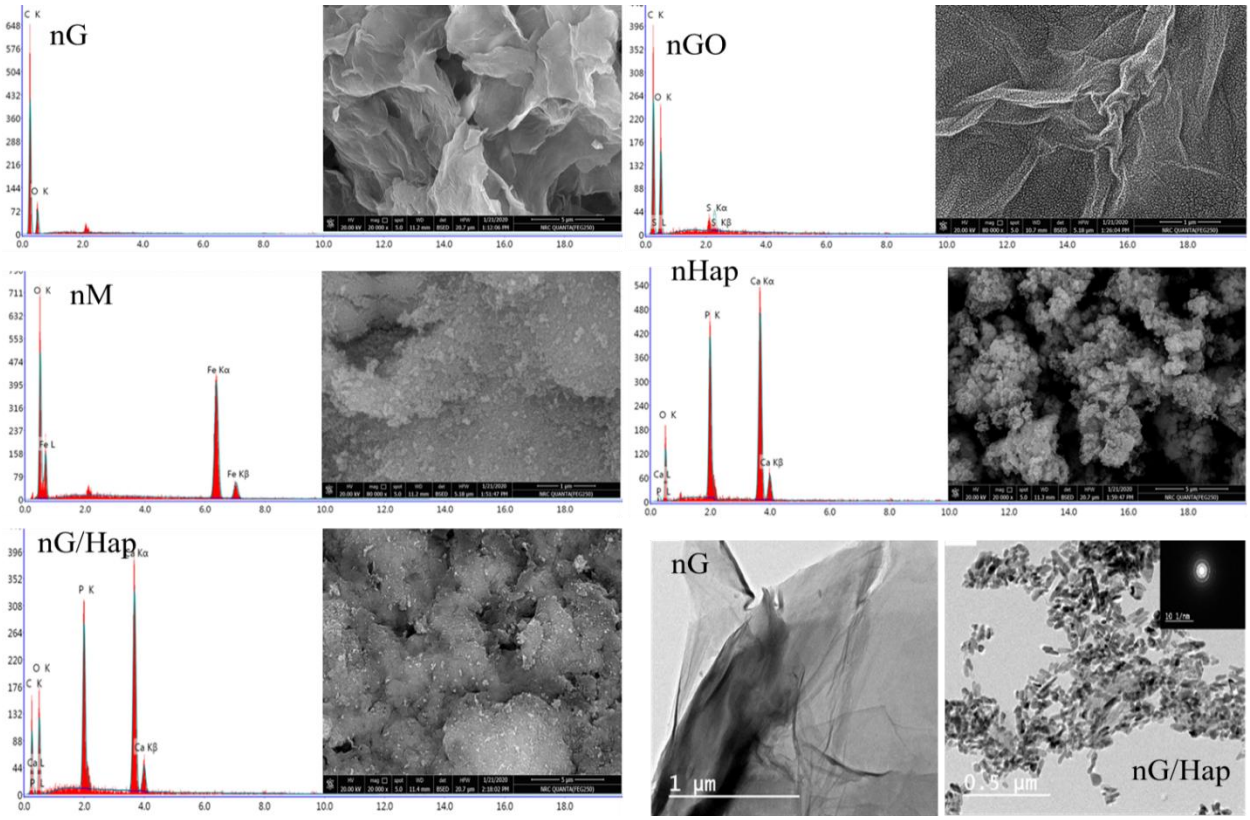

Fig. S2 scanning electron microscopy (SEM), and Energy dispersive X-ray (EDX) of graphene (nG), graphene oxide (nGO), magnetite (nM), hydroxyapatite (nHap) and graphene-hydroxyapatite (nG/Hap) and Transmission electron microscopy (TEM) images for graphene (nG) and graphene/hydroxyapatite diffraction (nG/Hap)

Table S1 energy dispersive X-ray (EDX) analysis of the solely and dual nanoparticles

Nanoparticle	Element	Weight %	Atomic %	Net Int.	Error %
Graphene (nG)	Carbon	70.4	76.01	99.85	5.83
	Oxygen	29.6	23.99	19.21	14.51
Graphene oxide (nGO)	Carbon	54.43	61.95	62.78	8.58
	Oxygen	43.52	37.18	40.94	12.71
	Sulfur	2.05	0.88	13.58	12.9
Magnetite (nM)	Oxygen	30.56	60.57	130.98	7.34
	Iron	69.44	39.43	201.84	3.08
Hydroxyapatite (NHap)	Oxygen	42.16	62.48	34.49	13.49
	Phosphorous	18.93	14.49	135.51	4.57
	Calcium	38.92	23.03	189.83	3.12
Graphene/hydroxyapatite (nG/Hap)	Carbon	28.48	42.49	23.75	12.62
	Oxygen	35.73	40.02	32.15	13.6
	Phosphorous	11.34	6.56	91.9	4.68
	Calcium	24.45	10.93	133.93	3.31

***Declaration of Interest Statement**

Declaration of interests

☒ The authors declare that they have no known competing financial interests or personal relationships that could have appeared to influence the work reported in this paper.

☐The authors declare the following financial interests/personal relationships which may be considered as potential competing interests: